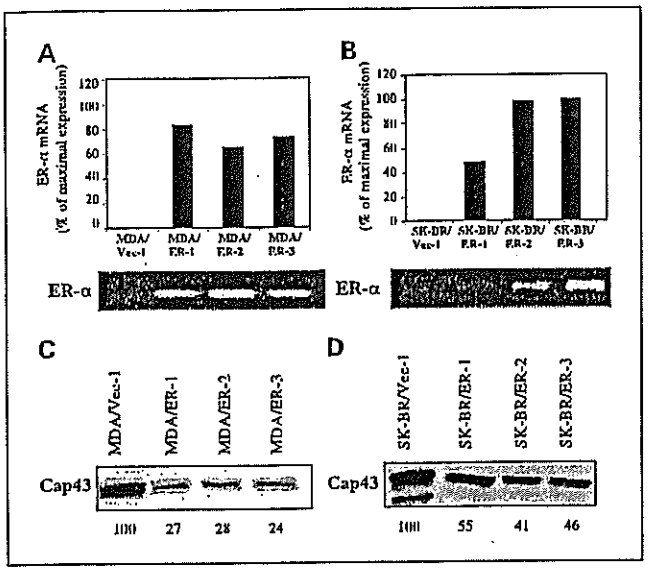

Fig. 6. Overexpression of ER-α in two breast cancer cell lines with low ER-α expression, MDA-MB-231 and SK-BR-3, and Cap43 expression in these cell lines. ER-α mRNA levels were determined by real-time PCR (*A* and *B*). Cap43 protein levels in ER-α transfectants were analyzed using Western blotting (*C* and *D*). Cap43 protein levels in each transfectant are normalized to the Cap43 protein band in MDA/Vec-1 or SK-BR/Vec-1 as 100%.

Effect of E_2 with or without tamoxifen or ICI 182780 on C-myc mRNA expression. C-myc as well as N-myc is known to regulate expression of *Cap43* gene (3). Expression of C-myc is highly susceptible to E_2. As shown in Fig. 5, expression of C-myc mRNA was markedly up-regulated by addition of E_2 in the ER-α-positive lines, T47D, MCF-7, and R-27. However, there was no change in *C-myc* expression in the ER-α-negative cell lines, SK-BR-3 and MDA-MB-231. Similarly, tamoxifen or ICI 182780 blocks this E_2-induced stimulatory effect in T47D and MCF-7 cells (Fig. 5). Compared with the inhibitory effect of tamoxifen on the E_2-induced C-myc up-regulation in MCF-7 cells, tamoxifen showed only a slight, if any, effect on the E_2-induced C-myc up-regulation in R-27 cells. By contrast, almost complete inhibition by ICI 182780 was observed on the E_2-induced up-regulation of C-myc in R-27 cells as well as MCF-7.

Overexpression of ER-α in ER-α-negative cells down-regulates Cap43 expression. We examined whether the E_2-induced down-regulation of Cap43 was specifically mediated through its interaction with ER-α. We introduced ER-α cDNA into the ER-α-negative lines, MDA-MB-231 and SK-BR-3, and established six cell lines, MDA/ER-1, MDA/ER-2, MDA/ER-3, SK-BR/ER-1, SK-BR/ER-2, and SK-BR/ER-3. We also isolated transfectants of the vector alone (MDA/Vec-1 and SK-BR/Vec-1). ER-α gene expression was observed in the cDNA transfectants from the SK-BR-3 and MDA-MB-231 lines (Fig. 6A and B). Three ER-α-expressing cell lines derived from SK-BR-3 and MDA-MB-231 showed a marked decrease in their expression of the Cap43 protein in comparison with their vector counterparts (Fig. 6C and D). Taken together, these data consistently indicated a close association between *Cap43* gene expression and E_2-ER-α signaling in human breast cancer cells.

Expression of Cap43 and ER-α in clinical samples of human breast cancer. We next performed immunohistochemical analysis to examine whether the expression of Cap43 was associated with ER-α expression in tissue samples from breast cancer patients. Ninety-six breast cancer patients were included in this study. The relationship between Cap43 expression and clinicopathologic findings is shown in Table 1. There was no significant correlation between the expression of Cap43 and age, tumor size, menopausal status, lymph node metastasis, EGFR expression, or HER-2 expression. However, because Cap43 expression was detected in 42% of grade 1 and 2 and 71% of grade 3 tumors, there was a significant correlation between Cap43 expression and tumor grade ($P = 0.0387$; Table 1). Univariate analysis for 5-year postoperative overall survival done on these patients showed that there was no significant difference in Cap43 expression according to the postoperative prognosis ($P = 0.345$).

Immunohistochemical analysis showed that breast cancers were variously positive and negative for the expression of Cap43 and ER-α. Figure 7 shows representative immunohistochemical data from two breast cancer patients. The tissue shown from case 1 with high expression of Cap43 and negligible expression of ER-α was therefore scored positive for the expression of Cap43 and negative for ER-α expression. By contrast, case 2 showed high expression of ER-α and negligible expression of Cap43, indicating that it was positive for ER-α and negative for Cap43. Positive expression of both Cap43 and ER-α was detected in 20 of 63 (31.7%) patients, and 43 of 63 (68.3%) patients were classified as being Cap43 negative and ER-α positive (Table 2). Cap43 expression was thus generally decreased in breast cancer cells from ER-α positive patients, and Cap43 expression was increased in breast cancer cells of ER-α-negative patients, indicating that the expression of Cap43 is inversely correlated with the expression of ER-α in breast cancer patients ($P = 0.0374$). On the other hand, there was no relationship between PgR and Cap43 expression in breast cancer patients ($P = 0.8405$; Table 2).

Table 1. Relationship between Cap43 expression and clinicopathologic variables in breast cancer ($n = 96$)

Factor	Total	Cap43 expression		*P*
		Negative, *n* (%)	Positive, *n* (%)	
Age		50.3 ± 12.1	51.2 ± 12.9	0.6629
Tumor size		3.7 ± 2.3	2.6 ± 1.3	0.1579
Menopausal status				
Pre	44	19 (43)	25 (57)	0.5432
Post	52	26 (50)	26 (50)	
Histologic grade				
1,2	55	32 (58)	23 (42)	0.0387
3	21	6 (29)	15 (71)	
Lymph node metastasis				
Absent	53	24 (45)	29 (55)	0.8375
Present	43	21 (49)	22 (51)	
EGFR				
Negative	73	38 (52)	35 (48)	0.0941
Positive	23	7 (30)	16 (70)	
HER-2				
Negative	62	29 (47)	33 (53)	>0.999
Positive	34	16 (47)	18 (53)	

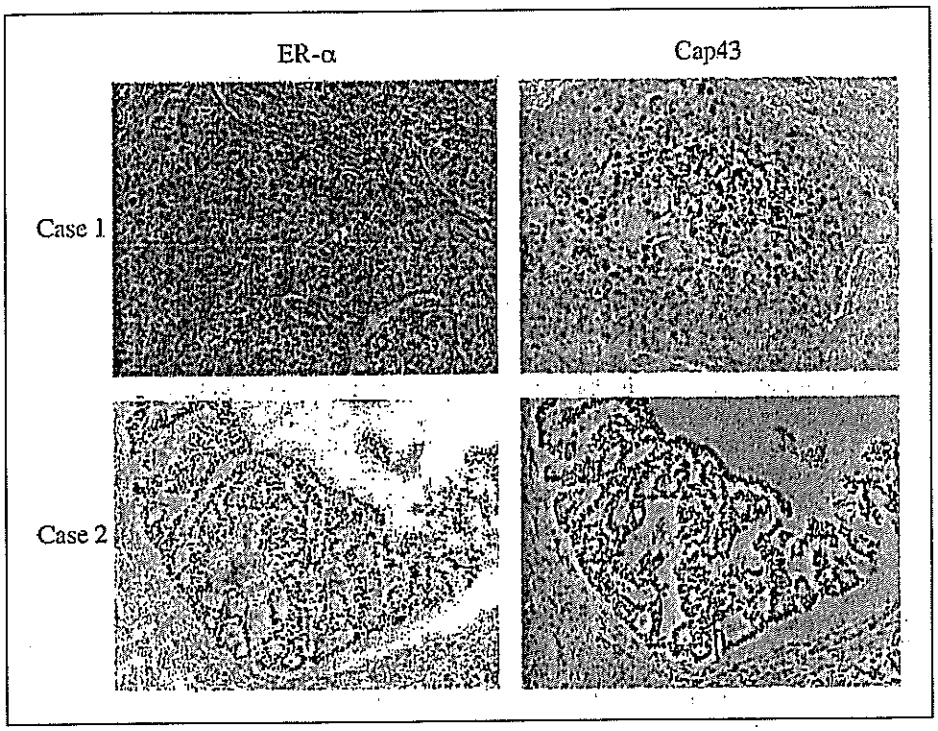

Fig. 7. Expression of Cap43 and ER-α in human breast cancer. Expression of Cap43 and ER-α in human breast cancer was analyzed by immunohistochemistry. Sections were analyzed for detection of ER-α (*left*) and the same site was also analyzed for Cap43 expression (*right*). Case 1 was evaluated as having high levels of Cap43 expression and not expressing ER-α. By contrast, case 2 showed high levels of ER-α expression and weak Cap43 expression. (Original magnification, ×200).

Discussion

In our present study, we observed that Cap43 expression levels were inversely correlated with expression levels of ER-α in all seven human breast cell lines (Fig. 1). One tamoxifen-resistant line, R-27, which was derived from the MCF-7 line, however, showed expression of both Cap43 and ER-α. The addition of E_2 was found to markedly down-regulate the expression of the *Cap43* gene in ER-α-positive cell lines but not in ER-α-negative lines (Fig. 3A and B). Because the expression of a representative ER-responsive gene, *pS2*, could be modulated by E_2 only in ER-α-positive lines (Fig. 3C), we concluded that ER-dependent signaling operated in these ER-α-positive cell lines but not in the ER-α-negative lines. Furthermore, overexpression of ER-α in ER-α-negative cell lines induced down-regulation of both protein and mRNA levels of Cap43. Exposure to nickel, however, markedly increased the expression of the *Cap43* gene in both ER-α-positive and ER-α-negative lines (Fig. 4), suggesting that the E_2-induced specific down-regulation of the Cap43 gene depends on ER-α. Taken together, these studies indicate that the presence of the functional ER-α could be required for E_2-induced down-regulation of Cap43.

We also showed that coadministration of tamoxifen or ICI 182780 abrogated the E_2-induced down-regulation of the *Cap43* gene in ER-α-positive lines. Expression of the *Cap43* gene is thus modulated in response to E_2 or antiestrogen possibly through the ER-α expressed in human breast cancer cells. Tamoxifen at 10^{-6} mol/L or ICI 182780 at 10^{-7} mol/L almost completely abrogated the E_2-induced down-regulation of Cap43 gene in ER-α-positive breast cancer cell lines, MCF-7 and T47D. The abrogatory effect of tamoxifen seemed to be much less in a tamoxifen-resistant subline, R-27, compared with the parental counterpart, MCF-7, in the presence of E_2 (10^{-8} to 10^{-6} mol/L). However, ICI 182780 could almost completely abrogate the E_2-induced down-regulation of Cap43 gene in R-27 cells. Moreover, the abrogatory effect of 10^{-6} mol/L tamoxifen on expression of the E_2-sensitive pS2 gene also seemed to be much less than that of ICI 182780 at 10^{-7} mol/L when R-27 cells were exposed to E_2 at 10^{-8} mol/L (Fig. 3C). ICI 182780 showed ~10-fold higher antiestrogenic activity in the regulation of *Cap43* as well as *pS2* gene compared with tamoxifen, and ICI 182780 could thus overcome tamoxifen resistance in breast cancer cells, consistent with previous reports (26, 27). Cap43 could be a molecular target for the functional hormone-dependent cell growth signal of breast cancers and also a target that is useful to determine the therapeutics efficacy of antiestrogenic anticancer agents.

Expression of *Cap43* gene is negatively regulated by *myc* gene (3). We examined the effect of E_2 on *C-myc* expression, and

Table 2. Relationship between Cap43 and hormone receptor expression in clinical samples ($n = 96$)

	Total	Cap43 expression		*P*
		Positive, *n* (%)	Negative, *n* (%)	
ER-α				
Positive	63	20/63 (31.7)	43/63 (68.3)	0.0374
Negative	33	21/33 (63.6)	12/33 (36.4)	
PgR				
Positive	50	26/50 (52.0)	24/50 (48.0)	0.8405
Negative	46	25/46 (54.3)	21/46 (45.7)	

E_2-induced up-regulation of *C-myc* gene was observed only in ER-α-positive breast cancer cell lines. E_2 thus up-regulated C-myc and down-regulated Cap43 possibly through the E_2-ER-α pathway. E_2-induced down-regulation of *Cap43* gene might be mediated through up-regulation of C-myc. However, further study should be required to determine how *C-myc* is involved in the E_2-induced down-regulation of Cap43 gene. Oncogenes, tumor suppressor genes, and several physiologic stimuli are known to modulate expression of Cap43 (see Introduction). Recent studies have shown that Cap43 is a p53 target gene (16, 17). Cap43 inhibited polyploidy in p53-negative cancer cell lines and increased the cell population at M phase when exposed to Taxol, a microtubule inhibitor, indicating that Cap43 plays a role in the p53-dependent mitotic spindle checkpoint (17). Stein et al. have also reported that Cap43 is necessary for p53-dependent apoptosis (16). Of the breast cancer cell lines used in this study, SK-BR-3, MDA-MB-231, and T47D have mutant p53 and MCF-7 has wild-type p53 (IARC TP53 Mutation Database, http://www-p53.iarc.fr/). Both ER-α-positive and ER-α-negative breast cancer cell lines with wild-type p53 showed a marked increase in Cap43 expression when exposed to doxorubicin, an anticancer agent that mediates cytotoxicity through p53.[6] Nickel also promoted the increased expression of Cap43 in all ER-α-positive and ER-α-negative lines (Fig. 4). The up-regulation of Cap43 by nickel or doxorubicin occurred irrespective of the presence of p53. Tamoxifen- and ICI 182780–induced abrogation of the E_2-induced down-regulation of Cap43 might also occur irrespective of the presence of the p53 pathway but does depend on the presence of ER-α.

Cap43 is a putative metastasis suppressor gene in human colon and prostate cancer, and its expression in these cancers is closely correlated with the prognosis of patients (18, 19). We also observed an inverse correlation between Cap43 expression and the prognosis of patients with pancreatic cancers.[7] Immunohistochemical studies by Bandyopadhyay et al. (20) on tissue from 85 breast cancer patients have shown that patients positive for Cap43 have a significantly more favorable prognosis than those with reduced expression of Cap43. The Cap43 protein was detected in normal mammary gland cells in all 85 breast cancer patients; but its expression was significantly reduced in the tumor cells of 30% of patients (20). In our present study, immunohistochemical analysis of breast cancers showed an inverse correlation between Cap43 expression and histologic grade or ER-α expression (Tables 1 and 2). However, there was no apparent correlation between Cap43 expression and other clinical and pathologic features, including lymph node metastasis and prognosis (Tables 1 and 2). At present, the reasons underlying discrepancies on the correlation between Cap43 expression and prognosis in breast cancer patients are unclear. Such discrepancies might be due to differences in the background of patients and the methods and evaluation of immunohistochemical staining used. There are also conflicting studies regarding the effects of Cap43 expression levels in colon cancer. Cap43 has been reported to be down-regulated in colon cancers with low levels of metastasis (4, 18). By contrast, a study by Wang et al. reported that Cap43 expression was well correlated with the progression of colon cancer (28). Further studies are required to understand the pathways by which Cap43 protein could modulate malignant characteristics and mechanisms, including tumor progression in breast cancer.

The action of estrogen is mediated by nuclear-localizing ER through the regulation of target gene transcription (i.e., genomic signaling). On the other hand, recent studies presented another pathway of so-called nongenomic signaling that is mediated by activation of membrane-associated ER. This nongenomic signaling events by membrane-associated ER could be also involved in some physiologic functions of E_2 (29–33). The E_2 concentrations that cause the maximal effect on the down-regulation of Cap43 in this study might be rather higher than physiologically most effective concentrations, suggesting that this E_2-induced down-regulation of Cap43 could be mediated through nongenomic signaling by membrane-associated ER. We, however, observed that most of ERs were localized in nucleus of the cells and we did not observe any apparent differences in the membrane localization of ER when the cells exposed to 10^{-12} to 10^{-6} mol/L E_2 by immunocytochemistry (data not shown). It is also known that nongenomic signaling by membrane-associated ER was not blocked by the pure antiestrogen ICI 182780 (29, 34, 35). Consistent with these findings, treatment with ICI 182780 effectively blocked the E_2-induced down-regulation of Cap43 in breast cancer cells (Fig. 3). Taken together, it seems unlikely that membrane-associated ER plays a critical role in the E_2-induced down-regulation of *Cap43* gene in our present study. However, further study is required to understand how E_2-dependent down-regulation of Cap43 is associated with genomic signaling.

In conclusion, the expression of *Cap43*, a putative differentiation- and metastasis-related gene, was greatly modulated by E_2 and/or antiestrogen in ER-α-positive breast cancer cells. Therefore, decreasing the susceptibility of Cap43 to antiestrogens would be a potential therapeutic strategy for the treatment of breast cancer.

[6] A. Fotovati, unpublished data.

[7] Y. Maruyama et al., unpublished data.

Acknowledgments

We thank Kenji Nakano and Fumihito Hosoi for fruitful discussions.

References

1. Zhou D, Salnikow K, Costa M. Cap43, a novel gene specifically induced by Ni^{2+} compounds. Cancer Res 1998;58:2182–9.
2. Agarwala KL, Kokame K, Kato H, Miyata T. Phosphorylation of RTP, an ER stress-responsive cytoplasmic protein. Biochem Biophys Res Commun 2000; 272:641–7.
3. Shimono A, Okuda T, Kondoh H. N-myc-dependent repression of ndr1, a gene identified by direct subtraction of whole mouse embryo cDNAs between wild type and N-myc mutant. Mech Dev 1999;83: 39–52.
4. van Belzen N, Dinjens WN, Diesveld MP, et al. A novel gene which is up-regulated during colon epithelial cell differentiation and down-regulated in colorectal neoplasms. Lab Invest 1997;77:85–92.
5. Kurdistani SK, Arizti P, Reimer CL, Sugrue MM, Aaronson SA, Lee SW. Inhibition of tumor cell growth by RTP/rit42 and its responsiveness to p53 and DNA damage. Cancer Res 1998;58:4439–44.
6. Kokame K, Kato H, Miyata T. Homocysteine-respondent genes in vascular endothelial cells identified by differential display analysis. GRP78/BiP and novel genes. J Biol Chem 1996;271:29659–65.

7. Salnikow K, Kluz T, Costa M. Role of Ca(2+) in the regulation of nickel-inducible Cap43 gene expression. Toxicol Appl Pharmacol 1999;160:127–32.
8. Park H, Adams MA, Lachat P, Bosman F, Pang SC, Graham CH. Hypoxia induces the expression of a 43-kDa protein (PROXY-1) in normal and malignant cells. Biochem Biophys Res Commun 2000;276:321–8.
9. Masuda K, Ono M, Okamoto M, et al. Down-regulation of Cap43 gene by von Hippel-Lindau tumor suppressor protein in human renal cancer cells. Int J Cancer 2003;105:803–10.
10. Nishie A, Masuda K, Otsubo M, et al. High expression of the Cap43 gene in infiltrating macrophages of human renal cell carcinomas. Clin Cancer Res 2001;7:2145–51.
11. Okuda H, Hirai S, Takaki Y, et al. Direct interaction of the β-domain of VHL tumor suppressor protein with the regulatory domain of atypical PKC isotypes. Biochem Biophys Res Commun 1999;263:491–7.
12. Lachat P, Shaw P, Gebhard S, van Belzen N, Chaubert P, Bosman FT. Expression of NDRG1, a differentiation-related gene, in human tissues. Histochem Cell Biol 2002;118:399–408.
13. Wakisaka Y, Furuta A, Masuda K, Morikawa W, Kuwano M, Iwaki T. Cellular distribution of NDRG1 protein in the rat kidney and brain during normal postnatal development. J Histochem Cytochem 2003;51:1515–25.
14. Okuda T, Higashi Y, Kokame K, Tanaka C, Kondoh H, Miyata T. Ndrg1-deficient mice exhibit a progressive demyelinating disorder of peripheral nerves. Mol Cell Biol 2004;24:3949–56.
15. Hirata K, Masuda K, Morikawa W, et al. N-myc downstream-regulated gene 1 expression in injured sciatic nerves. Glia 2004;47:325–34.
16. Stein S, Thomas EK, Herzog B, et al. NDRG1 is necessary for p53-dependent apoptosis. J Biol Chem 2004;279:48930–40.
17. Kim KT, Ongusaha PP, Hong YK, et al. Function of Drg1/Rit42 in p53-dependent mitotic spindle checkpoint. J Biol Chem 2004;279:38597–602.
18. Guan RJ, Ford HL, Fu Y, Li Y, Shaw LM, Pardee AB. Drg-1 as a differentiation-related, putative metastatic suppressor gene in human colon cancer. Cancer Res 2000;60:749–55.
19. Bandyopadhyay S, Pai SK, Gross SC, et al. The Drg-1 gene suppresses tumor metastasis in prostate cancer. Cancer Res 2003;63:1731–6.
20. Bandyopadhyay S, Pai SK, Hirota S, et al. Role of the putative tumor metastasis suppressor gene Drg-1 in breast cancer progression. Oncogene 2004;23:5675–81.
21. Nawata H, Bronzert D, Lippman ME. Isolation and characterization of a tamoxifen-resistant cell line derived from MCF-7 human breast cancer cells. J Biol Chem 1981;256:5016–21.
22. Kaplan EL, Meier P. Nonparametric estimation from incomplete observations. J Am Stat Assoc 1958;53:457–81.
23. Mizoguchi H, Uchiumi T, Ono M, Kohno K, Kuwano M. Enhanced production of tissue-type plasminogen activator by estradiol in a novel type variant of human breast cancer MCF-7 cell line. Biochim Biophys Acta 1990;1052:475–82.
24. Uchiumi T, Mizoguchi H, Hagino Y, Kohno K, Kuwano M. Counteraction of estradiol-induced activation of tissue-type plasminogen activator in a human breast cancer cell line by an anti-estrogen, LY117018. Int J Cancer 1991;47:80–5.
25. Vignon F, Capony F, Chambon M, Freiss G, Garcia M, Rochefort H. Autocrine growth stimulation of the MCF 7 breast cancer cells by the estrogen-regulated 52K protein. Endocrinology 1986;118:1537–45.
26. Hu XF, Veroni M, De Luise M, et al. Circumvention of tamoxifen resistance by the pure anti-estrogen ICI 182,780. Int J Cancer 1993;55:873–6.
27. Coopman P, Garcia M, Brunner N, Derocq D, Clarke R, Rochefort H. Anti-proliferative and anti-estrogenic effects of ICI 164,384 and ICI 182,780 in 4-OH-tamoxifen-resistant human breast-cancer cells. Int J Cancer 1994;56:295–300.
28. Wang Z, Wang F, Wang WQ, et al. Correlation of N-myc downstream-regulated gene 1 overexpression with progressive growth of colorectal neoplasm. World J Gastroenterol 2004;10:550–4.
29. Jacob J, Sebastian KS, Devassy S, et al. Membrane estrogen receptors: genomic actions and post transcriptional regulation. Mol Cell Endocrinol 2006;246:34–41.
30. Pawlak J, Karolczak M, Krust A, Chambon P, Beyer C. Estrogen receptor-α is associated with the plasma membrane of astrocytes and coupled to the MAP/Src-kinase pathway. Glia 2005;50:270–5.
31. Bulayeva NN, Wozniak AL, Lash LL, Watson CS. Mechanisms of membrane estrogen receptor-α-mediated rapid stimulation of Ca^{2+} levels and prolactin release in a pituitary cell line. Am J Physiol Endocrinol Metab 2005;288:E388–97.
32. Lu Q, Pallas DC, Surks HK, Baur WE, Mendelsohn ME, Karas RH. Striatin assembles a membrane signaling complex necessary for rapid, nongenomic activation of endothelial NO synthase by estrogen receptor α. Proc Natl Acad Sci U S A 2004;101:17126–31.
33. Xu Y, Traystman RJ, Hurn PD, Wang MM. Membrane restraint of estrogen receptor α enhances estrogen-dependent nuclear localization and genomic function. Mol Endocrinol 2004;18:86–96.
34. Heberden C, Reine F, Grosse B, et al. Detection of a raft-located estrogen receptor-like protein distinct from ER α. Int J Biochem Cell Biol 2006;38:376–91.
35. Ekstein J, Nasatzky E, Boyan BD, Ornoy A, Schwartz Z. Growth-plate chondrocytes respond to 17β-estradiol with sex-specific increases in IP3 and intracellular calcium ion signalling via a capacitative entry mechanism. Steroids 2005;70:775–86.

Tumor Growth Suppression in Pancreatic Cancer by a Putative Metastasis Suppressor Gene *Cap43/NDRG1/Drg-1* through Modulation of Angiogenesis

Yuichiro Maruyama,[1,3,4] Mayumi Ono,[4,5] Akihiko Kawahara,[2] Toshiro Yokoyama,[2] Yuji Basaki,[4] Masayoshi Kage,[2] Shigeaki Aoyagi,[1] Hisafumi Kinoshita,[1] and Michihiko Kuwano[3,4]

Departments of [1]Surgery and [2]Pathology, [3]Research Center for Innovative Cancer Therapy, Kurume University School of Medicine, Kurume, Japan, [4]Station-II for Collaborative Research, and [5]Department of Medical Biochemistry, Graduate School of Medical Sciences, Kyushu University, Fukuoka, Japan

Abstract

***Cap43* has been identified as a nickel- and calcium-induced gene, and is also known as N-myc downstream-regulated gene 1 (*NDRG1*), *Drg-1* and *rit42*. It is also reported that overexpression of Cap43 suppresses metastasis of some malignancies, but its precise role remains unclear. In this study, we asked how Cap43 could modulate the tumor growth of pancreatic cancer. Stable Cap43 cDNA transfectants of pancreatic cancer cells with Cap43 overexpression showed similar growth rates in culture as their control counterparts with low Cap43 protein level. By contrast, Cap43 overexpression showed a marked decrease in tumor growth rates *in vivo*. Moreover, a marked reduction in tumor-induced angiogenesis was observed. Gelatinolytic activity by matrix metalloproteinase-9 and invasive ability in Matrigel invasion activity were markedly decreased in pancreatic cancer cell lines with high Cap43 expression. Cellular expression of matrix metalloproteinase-9 and two major angiogenic factors, vascular endothelial growth factor and interleukin-8, were also significantly decreased in cell lines with Cap43 overexpression as compared with their parental counterparts. Immunohistochemical analysis of specimens from 65 patients with pancreatic ductal adenocarcinoma showed a significant association between Cap43 expression and tumor microvascular density (P = 0.0001) as well as depth of invasion (P = 0.0003), histopathologic grading (P = 0.0244), and overall survival rates for patients with pancreatic cancer (P = 0.0062). Thus, Cap43 could play a key role in the angiogenic on- or off-switch of tumor stroma in pancreatic ductal adenocarcinoma.** (Cancer Res 2006; 66(12): 6233-42)

Introduction

The *Cap43* gene has been identified as a nickel- and calcium-inducible gene (1), which is also identical to the described N-myc downstream-regulated gene 1 (*NDRG1*; ref. 2). This is one of the four closely related genes (*NDRG1-4*), the expression of which is down-regulated by c-myc or the N-myc/Max complex (2–5). Cap43 is also identical to the homocysteine-inducible gene, reduced in tumor cells (*RTP/rit42*; ref. 6), and to the differentiation-related gene-1 (*Drg-1*; ref. 7). The protein encoded by the *Cap43* gene has a molecular weight of 43 kDa, has three unique 10-amino acid tandem-repeat sequences at its COOH terminus, and is phosphorylated by protein kinase A (8).

Although various characteristics of Cap43 have been reported by several laboratories, its exact function remains unclear. *Cap43* gene expression is highly responsive to nickel, cobalt, oxidative stress, hypoxia, phorbol esters, vitamins A and D, steroids, histone deacetylase–targeting drugs, homocysteine, β-mercaptoethanol, tunicamycin, and lysophosphatidylcholine as well as oncogene (*N-myc* and *c-myc*), and tumor suppressor gene (*p53* and *VHL*) products (1, 2, 6, 9, 10). Cap43 is expressed in most organs—particularly the prostate, ovary, colon, and kidney—and its expression is markedly modulated during postnatal development in the kidney, brain, liver, and gut (2, 3, 11, 12), suggesting a key role for this gene in organ maturation. A nonsense mutation of human *Cap43* gene is causative for hereditary motor and sensory neuropathy-Lom (13). A relevant study by Okuda et al. established Cap43-deficient mice, and indicated that Cap43/NDRG1 is essential for the maintenance of the myelin sheaths in periphery nerves (14). Moreover, Cap43 expression was dramatically changed during the process of regeneration of periphery nerve system (15). Thus, Cap43 seems to play a key role in the development of the nervous system.

Concerning the plausible role of Cap43 in cancer progression, it was reported that overexpression of the *Cap43* gene results in the inhibition of growth in colon cancer cells as well as suppression of metastasis in prostate, colon, and breast cancer cells (16–18). *Cap43* gene expression is increased in many types of human tumors including colon, breast, prostate, kidney, liver, and brain cancers compared with normal tissue (19). By contrast, other groups have reported that expression of the *Cap43* gene is up-regulated in normal cells and in highly differentiated cancer cells, whereas it is down-regulated in poorly differentiated cancer cells in colon and prostate cancers (16, 17). Thus, Cap43 seems to play a critical role in both differentiation of normal tissue and progression of cancer. In our laboratory, we identified the *Cap43* gene as one of nine genes that were more highly expressed in cancerous compared with noncancerous regions of human renal tumors; we also observed high expression of Cap43 in macrophages infiltrating the stroma in renal cancer (20). Our previous study showed down-regulation of the *Cap43* gene in renal cancer cells by the *VHL* tumor suppressor gene (10). However, it remains unclear whether *Cap43* gene expression is associated with disease progression, prognosis, and malignant characteristics in human cancers other than prostate and breast cancer.

Pancreatic ductal adenocarcinoma is one of the most difficult neoplasms to treat curatively. Surgical resection is the standard

Requests for reprints: Michihiko Kuwano, Research Center for Innovative Cancer Therapy, Kurume University, 67 Asahi-machi, Kurume, Fukuoka 830-0011, Japan. Phone: 81-942-31-7888; Fax: 81-942-31-7888; E-mail: michik@med.kurume-u.ac.jp.

doi:10.1158/0008-5472.CAN-06-0183

treatment for this neoplasm, however, even after surgery, the majority of patients die within the first year after diagnosis (21). Overall 5-year survival rates for pancreatic cancers are <25% after radical surgery (22). It is difficult to predict which patient is at risk of early relapse following surgery, or which patient with advanced stage disease will show good long-term survival. K-ras point mutations and inactivation of p53, p16, and SMAD4 are often associated with malignant characteristics in pancreatic cancers, but mutations of K-ras and p53 are not significantly associated with the prognosis of patients with pancreatic cancer (21, 23, 24). In the prognosis of patients with pancreatic cancer, there seems to be a significant correlation between microvessel density and the expression of vascular endothelial growth factor (VEGF) and PD-ECGF in the tumor, as well as with E-cadherin, p27, PEDF, and SMAD4 expression (24–27). In this study, we investigated whether Cap43 expression could play any role in tumor growth and angiogenesis by pancreatic ductal adenocarcinoma. Moreover, we also asked if Cap43 could be associated with disease progression or the malignant properties of pancreatic ductal adenocarcinoma.

Materials and Methods

Materials and cell lines. Human pancreatic cancer cell lines were obtained as follows: BxPC-3, PANC-1, and MIApaca-2 were from the American Type Culture Collection (Manassas, VA); SUIT-2 was from T. Iwamura at the Miyazaki Medical College, Miyazaki, Japan (28); and KP-1 and KP-4 were from A. Kono at the National Kyushu Cancer Center, Fukuoka, Japan (29). All cell lines were maintained in DMEM supplemented with 10% fetal bovine serum (FBS) and incubated in a humidified atmosphere of 5% CO_2 at 37°C.

The rabbit polyclonal antibody against Cap43, which was raised by immunizing rabbits with a synthetic peptide corresponding to an internal sequence of human Cap43 coupled to keyhole limpet hemocyanin, was used as previously described (20). Other antibodies were purchased as follows: anti-β-actin antibody was from Abcam, Inc., (Cambridge, MA); anti-CD31 antibody was from PharMingen (San Diego, CA); and anti-CD34 antibody was from Nichirei (Tokyo, Japan).

Expression vector construction and transfection. Cap43 cDNA was amplified by reverse transcription-PCR (RT-PCR) using the 5′ and 3′ primers 5′-CATGTCTCGGGAGATGCAGGATG-3′ and 5′-AGGCCGCCTAGCAGGAGACC-3′, respectively. Amplified Cap43 cDNA was ligated into the pCR2.1-TOPO vector (Invitrogen, Carlsbad, CA) and transferred to the pIRESneo2 expression plasmid (pIRESneo2-Cap43). Cells were transfected with pIRESneo2-Cap43 or pIRESneo2 using LipofectAMINE 2000 (Invitrogen) following the manufacturer's protocol. Stable transfected clones were established using G418 selection.

Western blot analysis. Cells were rinsed with ice-cold PBS and lysed in buffer containing 50 mmol/L Tris-HCl, 350 mmol/L NaCl, 0.1% NP40, 5 mmol/L EDTA, 50 mmol/L NaF, 1 mmol/L phenylmethylsulfonyl fluoride, 10 μg/mL aprotinin, 10 μg/mL leupeptin, and 1 mmol/L Na_3VO_4. Cell lysates were subjected to SDS-PAGE and blotted onto Immobilon membranes (Millipore Corp., Bedford, MA) as described previously (10). After transfer, the membrane was incubated with blocking solution followed by primary antibody. Antibody detection was done using an enhanced chemiluminescence system (Amersham Biosciences Corp., Piscataway, NJ; ref. 30). The intensity of the luminescence was quantified using a CCD camera combined with an image analysis system (LAS-1000; Fuji Film, Japan).

Matrigel invasion assay. BD BioCoat Matrigel Invasion Chambers (BD Bioscience, Bedford, MA) were used according to the manufacturer's instructions. Pancreatic cancer cells (1×10^5) in serum-free DMEM containing 0.1% bovine serum albumin were seeded onto Matrigel-coated filters in the upper chambers. In the lower chambers, DMEM containing 10% FBS was added as a chemoattractant. After 24 hours of incubation, cells on the upper surface of the filters were removed with a cotton swab, and the filters were fixed with 100% methanol and stained with Giemsa dye (31). The cells that had invaded to the lower side of the filters were viewed under an Olympus microscope and counted in five fields of view. The invasive ability of the cancer cells was expressed as the mean number of cells in five fields. The assay was carried out as three independent experiments.

Gelatin zymography. Secreted metalloproteinases and their gelatinolytic activity were measured by zymography (32). Equal number of cells were plated on 24-well culture dishes and allowed to reach confluence over 24 hours. Cells were washed in PBS and incubated for 24 hours in 500 μL of serum-free DMEM. Conditioned media samples were then loaded onto 10% SDS-PAGE that had been copolymerized with 1 mg/mL of gelatin. Electrophoresis was done under nonreducing conditions. Gels were washed in 2.5% Triton X-100 for 30 minutes, and were incubated in collagenase buffer [100 mmol/L Tris-HCl (pH 8.0), 5 mmol/L $CaCl_2$, 0.02% NaN_3] for 40 hours at 37°C. Gels were stained for 30 minutes with 0.5% Coomassie blue and then destained (30% methanol and 10% acetic acid) thrice for 15 minutes. The presence of gelatinolytic activity due to secreted metalloproteinases was indicated by an unstained proteolytic region in the gel.

Quantitative real-time PCR analysis. Isolation of total cellular RNA was done as described previously (33). In brief, PCR amplification reaction mixtures (20 μL) contained cDNA, TaqMan Universal PCR Master Mix (Applied Biosystems, Foster City, CA), primer pairs, and probe. The primer pairs and probe were obtained from Applied Biosystems. Thermal cycle conditions included holding the reactions at 50°C for 2 minutes and at 95°C for 10 minutes, and cycling for 40 cycles between 95°C for 15 seconds and 60°C for 1 minute. Results were collected and analyzed with an ABI Prism 7300 Sequence Detector System using the comparative ΔCt methods. All data were controlled for quantity of RNA input by performing measurements on an endogenous reference gene (*GAPDH*).

Animals. All animal experiments were approved by the Committee on the Ethics of Animal Experiments in Kyushu University Graduate School of Medical Sciences, Japan. Male BALB/C mice (6-10 weeks old) were purchased from Kyudo Co., Ltd. (Tosu, Japan). Male athymic *nu/nu* mice 5 weeks of age, weighing 20 to 22 g, and specific pathogen–free, were obtained from Charles River Laboratories (Yokohama, Japan). Mice were housed in microisolator cages with 12-hour light/dark cycles. Water and food were supplied ad libitum. Animals were observed for signs of tumor growth, activity, feeding, and pain in accordance with the guidelines of the Harvard Medical Area Standing Committee on Animals.

Mouse dorsal air sac assay. This assay was carried out with 6- to 10-week-old male mice as previously described (34, 35). Cells (3×10^6) were suspended in 150 μL of DMEM containing 2% FBS, and was injected into a chamber, which consisted of a ring covered with Millipore filters (0.45 μm pore size, Millipore Corp.) on each side. This was implanted into an air sac produced by injecting 10 mL of air s.c. on the back of an anaesthetized mouse (50 mg/kg pentobarbital, i.p.) on day 0. On day 5, the chambers were removed from the s.c. fascia, and replaced with black rings of the same inner diameter as the chambers. Photographs of these sites were assessed by counting the number of newly formed vessels >3 mm in length within the area of the rings. The number of newly formed blood vessels were each scored on scales from 0 to 8. Results are expressed as mean ± SD.

Nude mouse xenograft models and determination of microvascular density. Cells were suspended in sterile PBS at a concentration of 10^8 cells/mL and 100 μL were injected s.c. into the right flank of the nude mice. Tumor size was measured by calipers in the largest diameter and at a perpendicular dimension in order to calculate the tumor area.

Tumors of nude mouse xenograft. Intratumoral microvessels were detected using a rat anti-mouse CD31 described previously (33). Tumors in nude mouse were removed, snap-frozen in optimum cutting temperature compound (SAKURA Finetechnical, Japan), and 6-μm sections were cut, air-dried, and fixed in cold acetone for 10 minutes. The sections were blocked with 3% bovine serum albumin and labeled at room temperature with rat anti-mouse CD31 for 1 hour, followed by biotinylated goat anti-rat IgG for 20 minutes. Intratumoral microvessels in human specimens were detected using a monoclonal antibody against the CD34 antigen

(monoclonal mouse anti-human CD34 antibody; Nitirei, Tokyo, Japan). In all samples, the mean value for the number of microvessels was calculated from four vascular hotspots. They were then assessed as the microvascular density (MVD) for each case. Only the CD34 staining in the tumor area was reviewed, and any endothelial cell cluster consisting of two or more cells was considered to be a single, countable microvessel. All counts were done by three independent observers without any knowledge of the corresponding clinicopathologic data.

Determination of VEGF and interleukin-8 by ELISA. The concentrations of VEGF and interleukin-8 (IL-8) in the conditioned medium and tissue lysates were measured using commercially available ELISA kits (31). Cells were plated in 24-well dishes in medium containing 10% FBS. When the cells reached subconfluence, the medium was replaced with DMEM containing 2% FBS, then the cells were incubated for 24 hours. Results were normalized for the number of cells and reported as picograms of growth factor/10^5 cells/24 hours. Tumors obtained from mice were homogenized in T-PER Tissue Protein Extraction reagent containing protein inhibitor cocktail (Pierce, Rockford, IL) and centrifuged at 13,000 × g for 10 minutes. The concentrations of VEGF and IL-8 in the supernatant of the lysates were measured by using an ELISA kit following the manufacturer's protocols.

Patients and specimens. Surgically resected specimens from 65 patients with pancreatic ductal adenocarcinomas were studied. All patients underwent surgical resection between 1991 and 1998 in the Department of Surgery at the Kurume University Hospital, Japan. Among these patients, 43 underwent pancreaticoduodenectomy, 21 underwent distal pancreatectomy, and one underwent total pancreatectomy. All subjects underwent extended radical lymphadenectomy. Pancreatic resection was not done in patients presenting with distant site metastasis. All cases of mucinous cystadenocarcinoma or intraductal papillary-mucinous carcinoma were excluded from our study. Pancreatic ductal adenocarcinoma tissues were obtained from 37 men and 28 women with a mean age of 64 years (age range, 40-80 years).

Immunohistochemical analysis of Cap43. All human specimens were fixed in 10% formalin and embedded in paraffin wax. Unstained 4-μm sections were then cut from paraffin blocks for immunohistochemical analysis. The sections were stained with rabbit anti-Cap43 polyclonal antibody (10, 20). Cap43-specific immunoreactivity was scored by estimating the percentage of labeled tumor cells as follows: score 0, no positive cells; score +, <30% positive cancer cells; score ++, 30% to 80% positive cancer cells; and score +++, >80% positive cancer cells. Specimens were considered positive for Cap43 expression when the score was ++ or +++, and were considered negative for Cap43 expression when the score was 0 or +. All procedures were done by two independent assessors and one pathologist, all of whom had no previous knowledge of the clinical outcome for this series of cases. Individual specimens with discordant results among the investigators were re-evaluated.

Statistical analysis. Data are expressed as mean ± SD. Comparisons between groups were done using Welch's t test. The Kaplan-Meier method was used to calculate the overall survival rate and the prognostic significance was evaluated by the log-rank test. The correlation of Cap43 immunoreactivity with the patients' clinicopathologic variables were analyzed by Fisher's exact test. Differences were considered significant at $P < 0.05$.

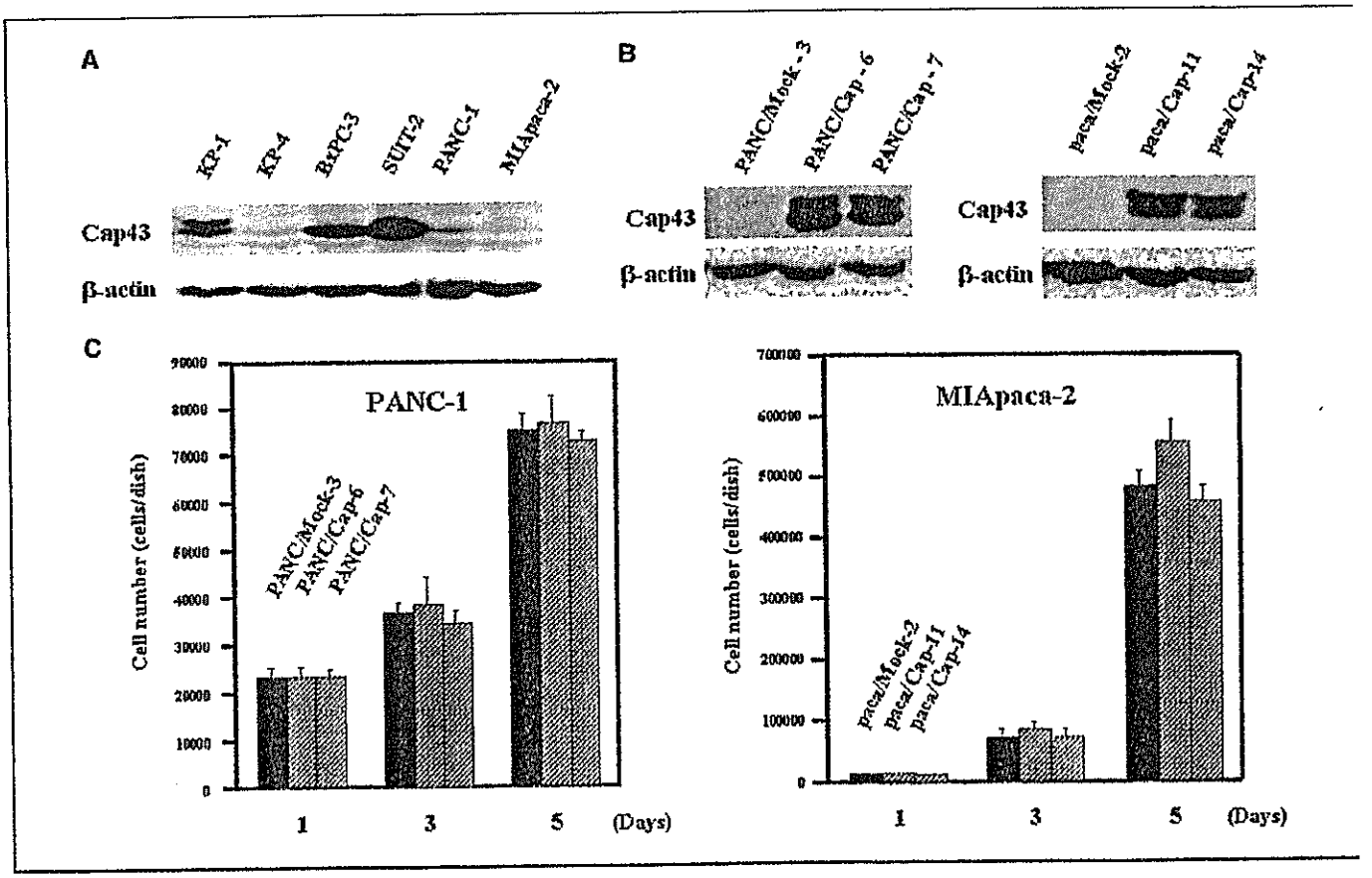

Figure 1. Effect of Cap43 expression levels and cell proliferation. *A*, expression of Cap43 in six pancreatic cancer cell lines was determined by Western blot analysis. *B*, expression of Cap43 in Cap43 transfectants or mock transfectants in two pancreatic cancer cell lines determined by Western blot analysis. *C*, comparison of cell growth between Cap43 transfectants and their mock transfectants in PANC-1 and MIApaca-2. Cell growth of various cell lines in DMEM containing 10% FBS was measured on days 1, 2, 3, 4, and 5, after seeding 2 ×10^4 cells/dish on day 0 in PANC-1 clones and after seeding 5 ×10^3 cells/dish on day 0 in MIApaca-2 clones. *Columns*, mean of three independent experiments; *bars*, ±SD.

Results

Cap43 levels had no effects on the cell proliferation rates of pancreatic cancer cells in culture. We first compared the protein levels of Cap43 in six pancreatic cancer cell lines. Of the six lines, KP-1, BxPC-3, and SUIT-2 showed relatively higher Cap43 expression, whereas KP-4, PANC-1, and MIApaca-2 showed relatively lower Cap43 expression (Fig. 1*A*). We next established cell lines that express higher amounts of Cap43 by transfection of Cap43 cDNA into two cell lines, PANC-1 and MIApaca-2. Two Cap43 cDNA transfectants from PNAC-1, PANC/Cap-6, and PANC/Cap-7, and those from MIApaca-2, paca/Cap-11, and paca/Cap-14, showed enhanced expression of Cap43 as compared with their parental mock transfectants, PANC/Mock-3 and paca/Mock-2, respectively (Fig. 1*B*). We also compared the growth rates of mock and Cap43 cDNA transfectants of PANC-1 and MIApaca-2 in the presence of 10% serum (Fig. 1*C*). No significant difference in growth rates was observed between their parental counterparts and transfected cell lines.

A marked decrease of tumor growth and angiogenesis by Cap43 overexpression in pancreatic cancer cells. We next examined whether overexpression of Cap43 could modulate tumor growth in mice under xenograft assay systems. The tumor growth of both paca/Cap-11 and paca/Cap-14 showed markedly reduced rates as compared with their mock-transfected line, paca/Mock-2 (Fig. 2*A* and *B*). We could not observe any tumor growth when PANC/Mock-3, PANC/Cap-6, and PANC/Cap-7 were transplanted. Determination of MVD showed much greater development of neovessels in paca/Mock-2 tumor than both paca/Cap-11 and paca/Cap-14 tumors (Fig. 2*C*). Quantitative analysis showed a significant decreasing number of MVD in both Cap43 transfectants by >50% of the control counterparts (Fig. 2*D*).

We compared the tumor-induced angiogenic activity of Cap43 cDNA transfectants and their mock transfectants in PANC-1 and MIApaca-2. Dorsal air sac assay showed the apparent development of new microvessels (*tn, arrowhead,* Fig. 3) with curled structures and many tiny bleeding spots by PANC/Mock-3 and paca/Mock-2, but only a slight, if any, development of such microvessels by their Cap43 cDNA transfectants (Fig. 3*A*). Quantitative analysis showed that the development of neovessels by both Cap43 cDNA

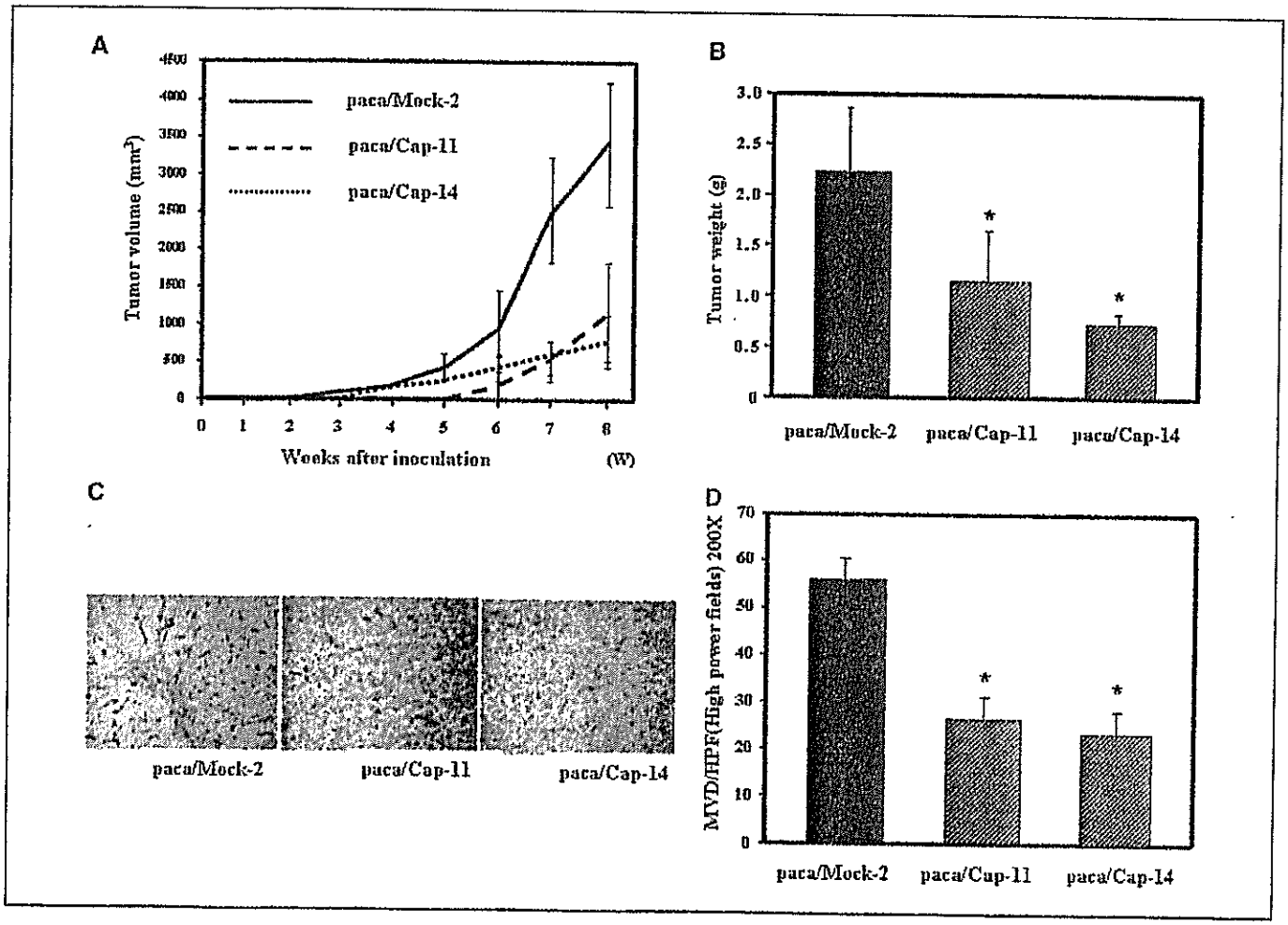

Figure 2. Comparison of tumor growth and angiogenesis between Cap43 transfectants and their mock transfectants. *A*, mean tumor volumes ± SD for groups of paca/Mock-2 (*black line*) or Cap43 transfectants (*dotted line*) implanted with 1×10^7 cells ($n = 8$). Tumor volumes were determined every week after tumor implantation. *B*, tumor weight data at 8 weeks from paca/Mock-2, paca/Cap-11, and paca/Cap-14 xenografts. *C*, representative photographs of tumor sections stained with anti-CD31 (MVD) from paca/Mock-2, paca/Cap-11, and paca/cap-14 xenografts at 8 weeks. *D*, the mean microvessel density for tumor sections from paca/Mock-2, paca/Cap-11, and paca/cap-14 xenograft at 8 weeks was determined by counting the number of CD31-positive vessels in high power fields (×200) of each section. *Columns*, mean; *bars*, ±SD; *, $P < 0.05$ significant difference between Cap43 transfectants and mock transfectant.

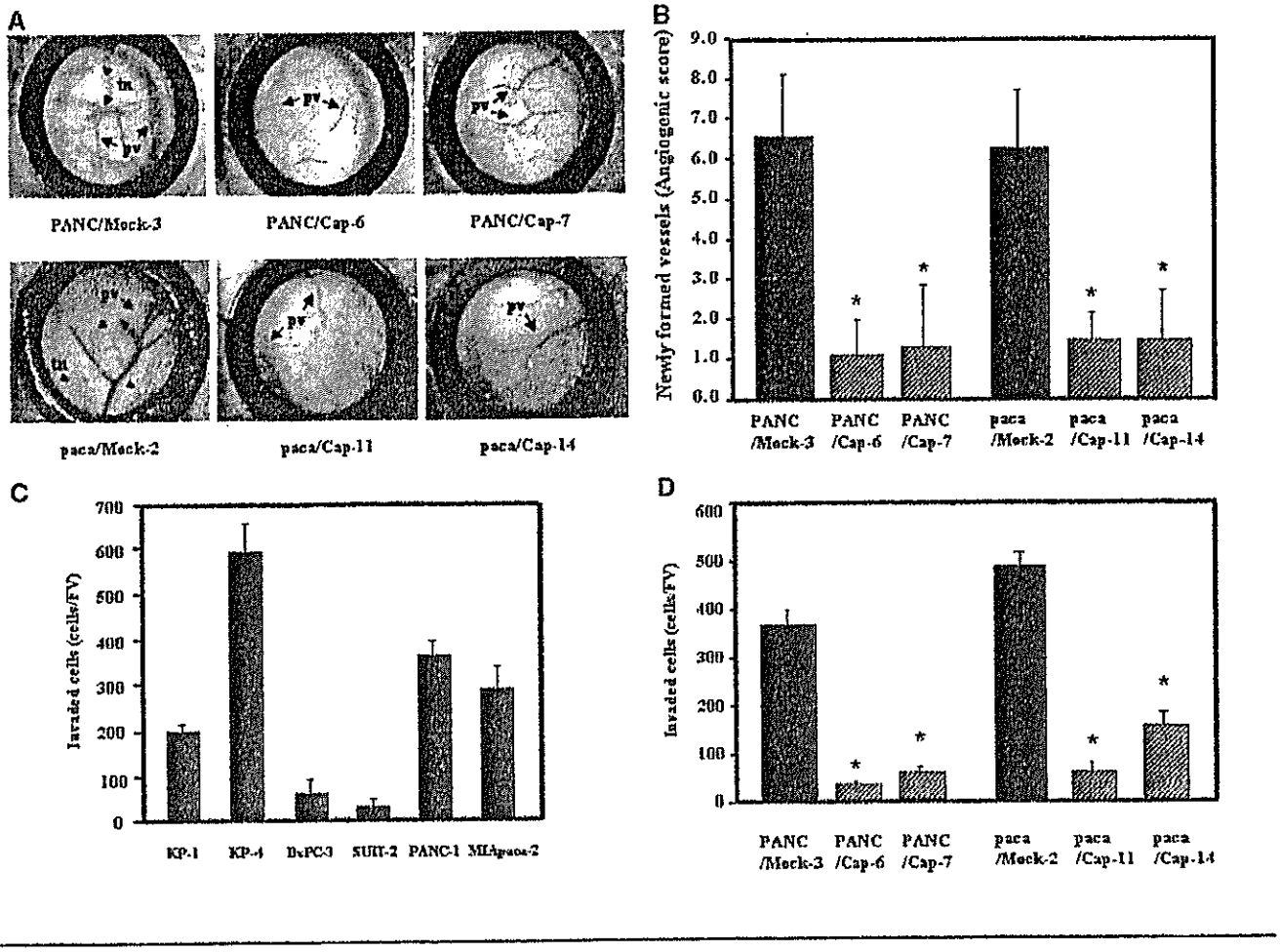

Figure 3. Effect of Cap43 overexpression on angiogenesis induced by pancreatic cancer cell lines in the mouse dorsal air sac assay and on invasive ability in Matrigel invasion assay: *A*, representative photographs of assay chambers containing Cap43 transfectants and their mock transfectants; *pv*, preexisting vessels; *tn*, tumor neovasculature. *B*, the angiogenic responses were determined by counting the number of new blood vessels (*tn*) >3 mm in length (*A* and *B*). *Columns*, mean for four or five mice; *bars*, ±SD; *, $P < 0.05$, significant difference between Cap43 transfectants and mock transfectant. *C*, comparison of the invasiveness of six human pancreatic cancer cell lines in the Matrigel invasion assay. Tumor cell invasiveness was quantified as the mean cell number of cells in five fields of view per filter (*cells/FV*). *Columns*, mean of three independent experiments; *bars*, ±SD. *D*, quantitative evaluation of invasiveness of the Cap43 transfectants and their mock transfectants in the Matrigel invasion assay. Tumor cell invasiveness was quantified as the mean cell number of invaded cells in five fields of view per filter (*cells/FV*). *Columns*, mean of three independent experiments; *bars*, ±SD; *, $P < 0.05$, significant difference between Cap43 transfectants and mock transfectant.

transfectants was <20% of their control counterparts in both MIApaca-2 and PANC-1 (Fig. 3*B*).

Effect of Cap43 on invasive ability in pancreatic cancer cells. We next examined if the expression of Cap43 could affect the cellular locomotion/invasion activity of pancreatic cancer cell lines by Matrigel invasion assay. Of the six cell lines, BxPC-3 and SUIT-2 showed relatively low invasive activity in comparison with the other four cell lines in photographs of Matrigel-coated filters (data not shown). Quantitative analysis showed a markedly lower invasive ability for two cell lines, BxPC-3 and SUIT-2, which expressed relatively high levels of Cap43 (see Fig. 1*A*), and intermediate invasiveness for one cell line, KP-1, which expressed a moderate Cap43 level (Fig. 3*C*). By contrast, three cell lines (KP-4, PANC-1, and MIApaca-2), which expressed relatively low Cap43 levels, showed higher invasive abilities. We further compared the invasive ability of Cap43 cDNA transfectants and their mock transfectants in PANC-1 and Miapaca-2. Two Cap43 transfectants consistently showed markedly decreased invasive ability compared with the mock transfectants in both PANC-1 and MIApaca-2 (Fig. 3*D*).

A marked effect of Cap43 on the expression of matrix metalloproteinase-9, VEGF, and IL-8. To determine why angiogenesis and cell locomotion/invasion are strongly affected by Cap43 expression, we compared the expression levels of angiogenesis-related factors, matrix metalloproteinases (MMP), VEGF, and IL-8 between Cap43 cDNA transfectants and their control counterparts. The expression of MMPs in cancer cells as well as vascular endothelial cells, regulate neovascularization by enhancement of pericellular fibrinolysis and cellular locomotion (36). Of the many MMPs, MMP-9 plays a critical role in the angiogenic switch during carcinogenesis (37). By using conventional gelatin zymography, we compared the activity of MMPs between Cap43-transfected lines and their control counterparts in PANC-1 and MIApaca-2. Two Cap43 transfectants, PANC/Cap-6 and PANC/Cap-7, which express high amounts of Cap43 protein showed much reduced MMP-9 activity (gelatinase B) compared

with their parental counterparts (PANC-1/Mock-3), whereas PANC/Cap-6 and -7 showed similar MMP-2 activities as its parental counterpart (Fig. 4*A*). We could not observe any apparent activity of MMP-2 and MMP-9 in cell lines derived from MIApaca-2 in this assay (data not shown). Both Cap43-overexpressing cell lines of PANC-1 showed <10% MMP-9 mRNA levels of that of PANC/Mock-3 (Fig. 4*B*). Although the mRNA levels of MMP-9 were ~10% in MIApaca-2 as compared with that in PANC-1, reduced levels of MMP-9 mRNA were also observed in Cap43-overexpressing cell lines of MIApaca-2 in comparison with their mock transfectant (Fig. 4*B*).

We also compared the cellular production of two potent angiogenic factors, VEGF and IL-8, by ELISA assay and reverse transcription-PCR between Cap43 cDNA transfectants and their control counterparts. Figure 4*C* showed a marked decrease in the production of VEGF in both PANC/Cap-6 and PANC/Cap-7 in comparison with PANC/Mock-3. However, we could not observe any apparent production of IL-8 in these lines derived from PANC-1, and also that of VEGF in cell lines derived from MIApaca-2, assayed by ELISA (data not shown). In contrast, cellular levels of IL-8 were ~10% and 60% in paca/Cap-11 and paca/Cap-14, respectively, of those in paca/Mock-2 (Fig. 4*C*). Determination of mRNA levels by quantitative real-time PCR also showed the marked decrease in cellular mRNA levels of both VEGF and IL-8 in Cap43 cDNA transfectants as compared with their parental counterparts in both PANC-1 and MIApaca-2 (Fig. 4*D*).

We further compared the production of VEGF and IL-8 in the s.c. tumors under *in vivo* conditions. Determination of mRNA levels by quantitative real-time PCR showed 12- and 18-fold increases in Cap43 mRNA levels in paca/Cap-14 tumor 1 and tumor 2, respectively, over those in paca/Mock-2 tumor when tumors were removed at 8 weeks after inoculation. We determined the expression levels of VEGF and IL-8 in tumors by ELISA assay system (see Materials and Methods). VEGF expression levels (pg/mg protein) were not detectable in both paca/Cap-14 tumor 1 and 2 when those were 280 ± 8.9 in paca/Mock-2 tumor. IL-8 expression levels (pg/mg protein) were 142 ± 10.2 and 46 ± 8.4 in paca/Cap-14 tumor 1 and tumor 2, respectively, when those were 580 ± 82.4 in paca/mock-2 tumor.

Association of Cap43 expression with angiogenesis and clinicopathologic characteristics as well as prognosis in patients with pancreatic cancer. The expression of immunoreactive Cap43 was examined immunohistochemically in resected specimens of 65 patients with pancreatic ductal adenocarcinoma. Two clinical examples of positive immunostaining (*a* and *b*) and two examples of negative immunostaining (*c* and *d*) are presented in Fig. 5*A*. Based on this immunohistochemical staining for Cap43, we classified the 65 cancer specimens into positive (n = 27) and negative (n = 38) groups. We further investigated whether Cap43 expression in patients with pancreatic ductal adenocarcinoma was associated with clinicopathologic variables such as age, gender, depth of invasion, lymph node metastasis, pathologic stage, and

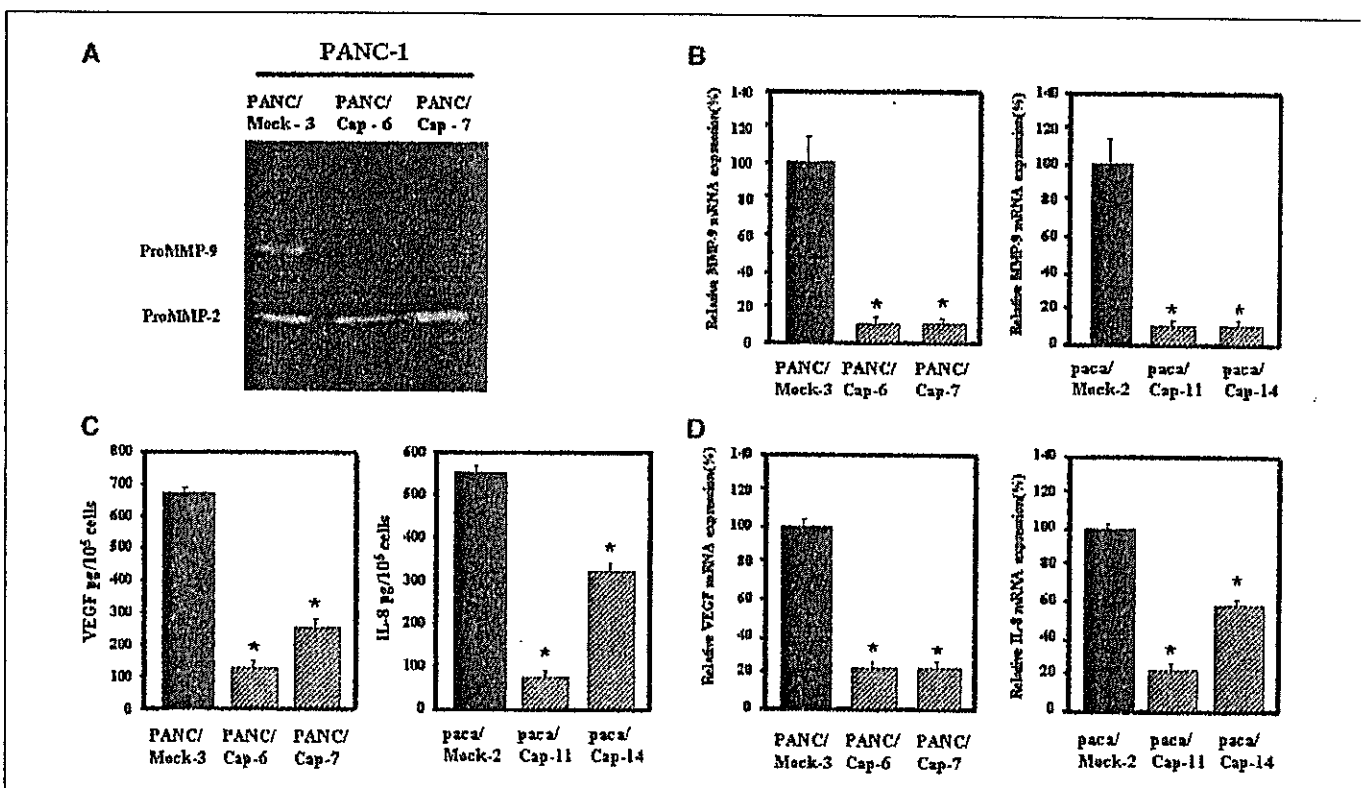

Figure 4. Effect of Cap43 on expression of MMP-9, VEGF, and IL-8. *A*, comparison of gelatinase activities in Cap43 transfectants and mock transfectant in PANC-1. Gelatin zymography for culture media of pancreatic cancer cell lines with or without Cap43 overexpression. *B*, expression of MMP-9 mRNA levels in Cap43 transfectants and their mock transfectants. Real-time PCR was done to determine MMP-9 mRNA levels. Expression was normalized to GAPDH mRNA levels (*, $P < 0.05$ versus mock transfectants). *C*, comparison of VEGF and IL-8 protein production between Cap43 transfectants and their parental counterparts for 24 hours by ELISA assay. *Columns*, mean of cultures in triplicate and have been normalized to account for cell numbers; *bars*, ±SD; *, $P < 0.05$ versus mock transfectants. *D*, expression of VEGF mRNA levels and IL-8 mRNA levels in Cap43 transfectants and their mock transfectants. Real-time reverse transcription-PCR was done to determine MMP-9 mRNA levels. Expression was normalized to GAPDH mRNA levels (*, $P < 0.05$ versus mock transfectants).

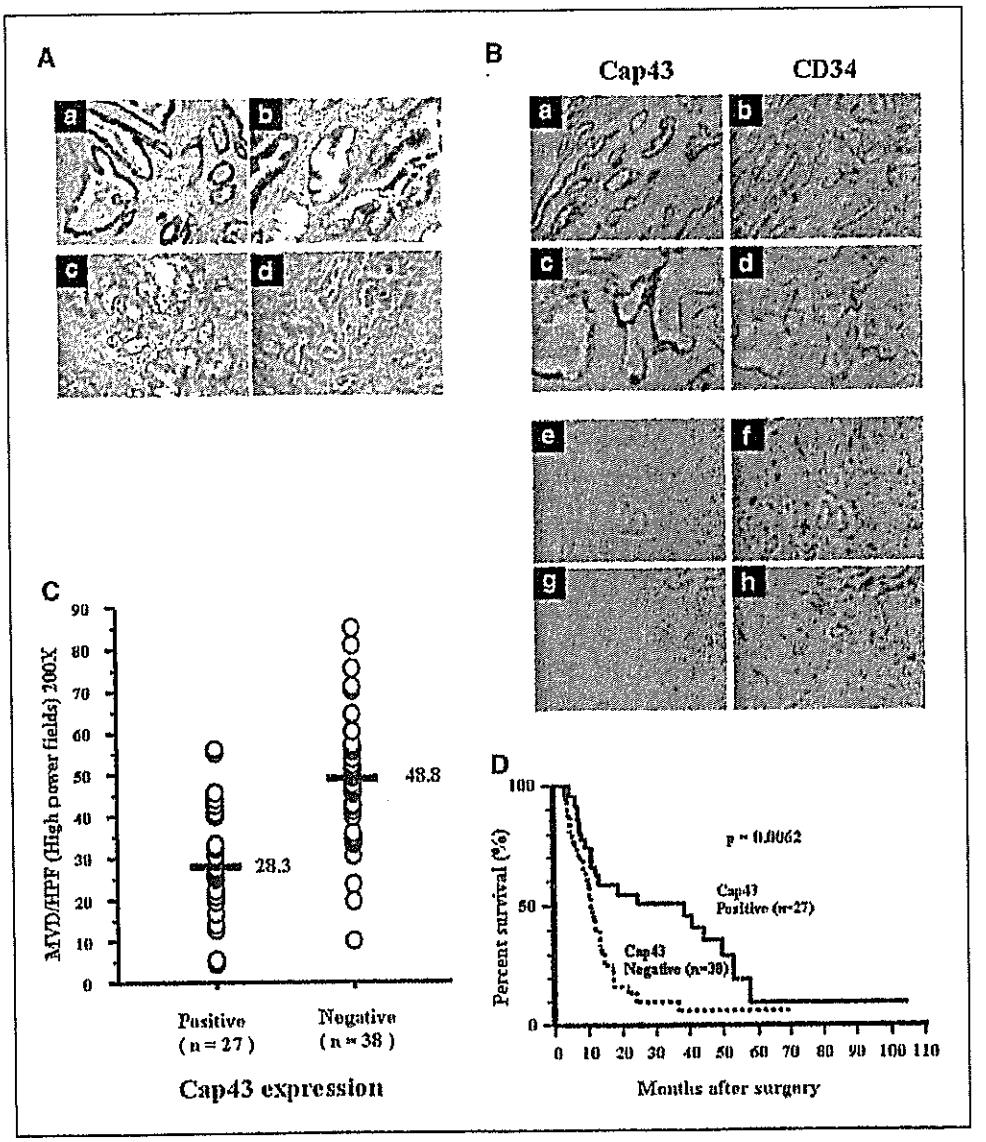

Figure 5. Correlation between Cap43 expression and MVD. Immunohistochemical analysis of Cap43 and microvessels in pancreatic ductal adenocarcinoma with anti-Cap43 and CD34 antibody (*A* and *B*). *A*, two clinical samples of patients with pancreatic ductal adenocarcinoma who had good long-term survival after surgery showing Cap43 expression (*a* and *b*). Two clinical samples of patients with pancreatic ductal adenocarcinoma who had poor survival after surgery showing reduced Cap43 expression (*c* and *d*). Original magnification, ×100. *B*, ductal adenocarcinoma cells in Cap43 positive specimens (*a* and *c*), and in Cap43-negative specimens (*e* and *g*). Immunohistochemical staining of anti-CD34 antibody. A tumor area with low vessel density (*b* and *d*) and high vessel density (*f* and *h*) are shown. Original magnification, ×100. *C*, correlation between Cap43 expression and MVD. The median value of MVD in a Cap43-negative specimen was 48.8 and in a Cap43-positive specimen was 28.3. *D*, Kaplan-Meier analysis of overall survival according to Cap43 expression levels in pancreatic ductal adenocarcinoma. The survival of patients whose cancer cells did not express Cap43 was significantly ($P = 0.0062$) worse than that of patients whose cancer cells expressed Cap43. Patients with Cap43-positive cancer ($n = 27$) and those with reduced expression of Cap43 ($n = 38$).

histopathologic grading. Cap43 expression was significantly correlated with depth of invasion ($P = 0.0003$), pathologic stage ($P = 0.0263$), and histopathologic grading ($P = 0.0244$), but not with lymph node metastasis (Table 1). We also determined MVD in tumors by immunostaining analysis with anti-CD34 antibody. Two clinical samples of Cap43-positive immunostaining with lower MVD (scoring number, <40; *a-d*) and two clinical samples of Cap43-negative immunostaining with higher MVD (scoring number, >40; *e-h*) are presented in Fig. 5*B*. Based on this immunohistochemical analysis, we classified patients into high (scoring number, >40; $n = 33$) and low (scoring number, <40; $n = 32$) MVD groups. High MVD was found to be significantly associated with negative Cap43 expression, whereas low MVD was significantly associated with positive Cap43 expression ($P = 0.0001$; Table 1). The median values of MVD in Cap43-positive specimens was 28.3, and those of MVD in Cap43-negative specimens was 48.8 (Fig. 5*C*). Immunohistochemical analysis of clinical specimens therefore suggested that high Cap43 expression was closely associated with low angiogenic status of pancreatic ductal adenocarcinoma.

Finally, we investigated whether Cap43 expression was associated with the prognosis for patients with pancreatic ductal adenocarcinoma. Kaplan-Meier analysis indicated that Cap43 protein expression showed a statistically significant correlation with survival after radical surgery ($P = 0.0062$; Fig. 5*D*), with cases lacking Cap43 expression having unfavorable prognoses. The median survival time for patients with tumors that were positive for Cap43 expression was 24.7 months, compared with 10.9 months for patients with tumors negative for Cap43 expression.

Discussion

Overexpression of Cap43 did not alter the growth rates of human prostate and colon cancer cells (16, 17). Consistent with these studies, cellular proliferation assay of Cap43-overexpressing cell lines of MIApaca-2 and PANC-1 showed similar growth rates as their parental counterparts in culture. Tumor growth *in vivo* showed a marked decrease by Cap43 overexpression in MIApaca-2 when their parental counterparts showed high tumor growth rates. Thus, Cap43 overexpression seemed to specifically affect tumor

Table 1. Association between Cap43 expression and clinicopathologic variables in 65 patients with pancreatic ductal adenocarcinoma

Variable	No. of patients	Cap43 expression		P^*
		Positive (n = 27)	Negative (n = 38)	
Age (y)				0.6760
<65	29	12	17	
≥65	36	15	21	
Gender				0.0868
Male	37	12	25	
Female	28	15	13	
Depth of invasion				0.0003†
T_1, T_2	24	17	7	
T_3, T_4	41	10	31	
Lymph node metastasis				0.5358
Negative	31	13	18	
Positive	34	14	20	
Pathologic stage				0.0263†
I	10	7	3	
II	4	2	2	
III	30	14	16	
IV	21	4	17	
Histopathologic grading				0.0244†
G_1	28	16	12	
G_2, G_3	37	11	26	
Microvascular density				0.0001†
Low (<40)	32	21	11	
High (>40)	33	6	27	

*Analyses were carried out using Fisher's exact test.
†$P < 0.05$ considered statistically different.

growth *in vivo* but not cell growth *in vitro*, suggesting the critical role of Cap43 in the modulation of tumor stroma in pancreatic cancer. Previous studies using animal experimental models have shown that Cap43 overexpression suppresses metastasis by prostate and colon cancer cells, suggesting that *Cap43/NDRG1* is a metastasis suppressor gene (16, 17). A relevant study by Bandyopadhyay et al. have reported that the Cap43/Drg-1 protein was significantly reduced in breast cancer cells, particularly, in patients with lymph node or bone metastasis as compared to those with localized breast cancer (18). Cap43 could thus affect not only metastasis/invasion but also tumor growth, suggesting that *Cap43/NDRG1* could be a putative metastasis suppressor gene. Concerning the possible mechanism for up-regulation of Cap43, Le and Richardson have previously reported that treatment of breast cancer cells by iron chelator with high antiproliferation activity up-regulates the expression of *Cap43/NDRG1* gene through hypoxia-inducible factor-1α–dependent and –independent pathways (38). Our recent study showed estradiol induced down-regulation of *Cap43* gene in estradiol receptor–positive breast cancer cell lines, and also that Cap43 expression was inversely correlated with the expression of estradiol receptor-α but not with progesterone receptor in human breast cancer (39). Thus, expression of Cap43 in breast cancer seems to be greatly affected under various conditions including hypoxia, metals, and estradiol.

Cap43 in cancer cells might alter the tumor stroma microenvironment, resulting in a block of tumor progression. Consistent with this notion, our present study further showed a marked decrease in angiogenesis by Cap43 overexpression in MIApaca-2 or PANC-1 in the dorsal air sac assay, and also decreased MVD in tumor induced by Cap43 overexpression in MIApaca-2 as compared with their parental counterparts. Cellular production of angiogenesis-related factors such as MMP-9, VEGF, and IL-8 were markedly reduced in cell lines with Cap43 overproduction. In gelatin zymography, there seemed to be almost no MMP-9 activity in PANC/Cap-6 and PANC/Cap-7 when their parental counterpart had MMP-9 activity. Although there was no apparent activity corresponding with MMP-9 and MMP-2 in cell lines of MIApaca-2, MMP-9 mRNA level was also reduced in both Cap43 transfectants of MIApaca-2. In the Matrigel invasion assay, pancreatic cancer cell lines with relatively higher Cap43 expression showed lower invasive ability. Cap43 overexpression may reduce both the expression and activity of MMP-9, resulting in altered cellular locomotion and invasive ability. A relevant study by Bergers et al. has reported that MMP-9 triggers the angiogenic switch during carcinogenesis of pancreas in transgenic mice (37). In this study, genetic ablation of MMP-9, but not that of MMP-2, impairs the induction of angiogenesis. Moreover, expression of two representative angiogenic factors, VEGF and IL-8, was also markedly reduced in cell lines overexpressing Cap43. Cellular production of VEGF and IL-8 was also inversely correlated with Cap43 levels. VEGF and IL-8 production was markedly decreased in the subcutaneous tumor by *Cap43* gene transfectant in comparison with tumors of the parental counterpart, suggesting that expression of VEGF and IL-8 is affected in both *in vitro* and *in vivo* conditions by Cap43 in pancreatic cancer. The low tumor angiogenic activity by Cap43 overexpression could be due to decreased expression of angiogenic factors such as VEGF, IL-8, and MMP-9. A more precise study should be required to understand the underlying mechanism of how the expression of such angiogenesis-related factors could be modulated by Cap43.

Consistent with previous studies (22, 40, 41), we found that the survival rates for 65 patients with pancreatic cancer were significantly correlated with histopathologic grading and depth of invasion. We further observed a close association between low Cap43 expression and poor prognosis in pancreatic ductal adenocarcinoma. Cap43 was originally isolated as a differentiation-related gene and is mostly expressed in differentiated epithelial cells (9, 11), and this might be relevant to its association with the histopathologic grading of pancreatic cancer. To our surprise, high MVD in clinical specimens of pancreatic cancer was found to be significantly associated with low Cap43 expression levels (Table 1; Fig. 5), consistent with our experimental animal model for tumor growth and MVD. On the other hand, poor prognosis and malignant progression are often significantly associated with VEGF and PD-ECGF, as well as with MVD in tumors (see Introduction). From our present study, MVD in clinical specimens of pancreatic cancer was also significantly associated not only with Cap43 (see Table 1) but also with prognosis of patients.[6] Pancreatic tumor growth is regulated by positive and negative angiogenesis modulators (42), and kinase inhibitors of both VEGF and EGF receptors were found to reduce the tumor

[6] Unpublished data.

growth and metastasis of pancreatic cancers in a xenograft model (43). Clinical studies also showed a close association of angiogenesis and/or enhanced expression of VEGF and other angiogenic factors with disease progression and patient survival in pancreatic cancers (44–46). Shi et al. have reported that IL-8 expression renders pancreatic cancer cells more tumorigenic and metastatic under various microenvironmental changes including hypoxia and acidosis (47). On the other hand, infiltration of tumor-associated macrophages is often closely associated with angiogenesis in various human malignancies (48, 49), and our previous study showed the expression of Cap43 in tumor-associated macrophages in human renal cancers (20). We also observed the expression of Cap43 in macrophages as well as cancer cells in pancreatic cancers when clinical specimens were examined by immunohistochemical analysis (data not shown). The role of Cap43 in macrophages, however, remains to be further studied.

In conclusion, we first demonstrated that Cap43 could switch-off angiogenesis and cell locomotion/invasion by pancreatic cancer cells. A putative metastasis suppressor function of Cap43/NDRG1 might be due to such modulation of angiogenesis in tumor stroma. Cap43 could be a novel target for angiogenesis and malignant characteristics of pancreatic cancers. How Cap43 could control the expression of angiogenesis-related genes in pancreatic cancer cells is now in progress in our laboratory.

Acknowledgments

Received 1/19/2006; revised 3/28/2006; accepted 4/17/2006.

Grant support: 21st Century COE Program for Medical Science, and by Health and Labour Sciences Research Grants of Third Term Comprehensive Control Research for Cancer from the Ministry of Health, Labour, and Welfare, Japan.

The costs of publication of this article were defrayed in part by the payment of page charges. This article must therefore be hereby marked *advertisement* in accordance with 18 U.S.C. Section 1734 solely to indicate this fact.

We thank A. Jimi, T. Fujii, and K. Shirouzu (Kurume University, Japan), S. Ueda, T. Kuwano, K. Masuda, A. Hirata, Y. Oda, and T. Eguchi (Kyushu University, Japan), and S. Jimi (Miyazaki University, Japan) for fruitful discussions. We also thank N. Shinbaru (Kyushu University) for preparing this manuscript.

References

1. Zhou D, Salnikow K, Costa M. Cap43, a novel gene specifically induced by Ni2+ compounds. Cancer Res 1998;58:2182–9.
2. Shimono A, Okuda T, Kondoh H. N-myc-dependent repression of ndr1, a gene identified by direct subtraction of whole mouse embryo cDNAs between wild type and N-myc mutant. Mech Dev 1999;83:39–52.
3. Okuda T, Kondoh H. Identification of new genes ndr2 and ndr3 which are related to Ndr1/RTP/Drg1 but show distinct tissue specificity and response to N-myc. Biochem Biophys Res Commun 1999;266:208–15.
4. Zhou RH, Kokame K, Tsukamoto Y, Yutani C, Kato H, Miyata T. Characterization of the human NDRG gene family: a newly identified member, NDRG4, is specifically expressed in brain and heart. Genomics 2001;73: 86–97.
5. Qu X, Zhai Y, Wei H, et al. Characterization and expression of three novel differentiation-related genes belong to the human NDRG gene family. Mol Cell Biochem 2002;229:35–44.
6. Kurdistani SK, Arizti P, Reimer CL, Sugrue MM, Aaronson SA, Lee SW. Inhibition of tumor cell growth by RTP/rit42 and its responsiveness to p53 and DNA damage. Cancer Res 1998;58:439–44.
7. van Belzen N, Dinjens WN, Diesveld MP, et al. A novel gene which is up-regulated during colon epithelial cell differentiation and down-regulated in colorectal neoplasms. Lab Invest 1997;77:85–92.
8. Agarwala KL, Kokame K, Kato H, Miyata T. Phosphorylation of RTP, an ER stress-responsive cytoplasmic protein. Biochem Biophys Res Commun 2000;272:641–7.
9. Kokame K, Kato H, Miyata T. Homocysteine-respondent genes in vascular endothelial cells identified by differential display analysis. GRP78/BiP and novel genes. J Biol Chem 1996;271:29659–65.
10. Masuda K, Ono M, Okamoto M, et al. Down-regulation of Cap43 gene by von Hippel-Lindau tumor suppressor protein in human renal cancer cells. Int J Cancer 2003;105:6803–10.
11. Lachat P, Shaw P, Gebhard S, van Belzen N, Chaubert P, Bosman FT. Expression of NDRG1, a differentiation-related gene, in human tissues. Histochem Cell Biol 2002;118:399–408.
12. Wakisaka Y, Furuta A, Masuda K, Morikawa W, Kuwano M, Iwaki T. Cellular distribution of NDRG1 protein in the rat kidney and brain during normal postnatal development. J Histochem Cytochem 2003;51: 1515–25.
13. Kalaydjieva L, Gresham D, Gooding R, et al. N-myc downstream-regulated gene 1 is mutated in hereditary motor and sensory neuropathy-Lom. Am J Hum Genet 2000;67:47–58.
14. Okuda T, Higashi Y, Kokame K, Tanaka C, Kondoh H, Miyata T. Ndrg1-deficient mice exhibit a progressive demyelinating disorder of peripheral nerves. Mol Cell Biol 2004;24:3949–56.
15. Hirata K, Masuda K, Morikawa W, et al. N-myc downstream-regulated gene 1 expression in injured sciatic nerves. Glia 2004;47:325–34.
16. Guan RJ, Ford HL, Fu Y, Li Y, Shaw LM, Pardee AB. Drg-1 as a differentiation-related, putative metastatic suppressor gene in human colon cancer. Cancer Res 2000;60:749–55.
17. Bandyopadhyay S, Pai SK, Gross SC, et al. The Drg-1 gene suppresses tumor metastasis in prostate cancer. Cancer Res 2003;63:1731–6.
18. Bandyopadhyay S, Pai SK, Hirota S, et al. PTEN up-regulates the tumor metastasis suppressor gene Drg-1 in prostate and breast cancer. Cancer Res 2004;64:7655–60.
19. Cangul H, Salnikow K, Yee H, Zagzag D, Commes T, Costa M. Enhanced expression of a novel protein in human cancer cells: a potential aid to cancer diagnosis. Cell Biol Toxicol 2002;18:87–96.
20. Nishie A, Masuda K, Otsubo M, et al. High expression of the Cap43 gene in infiltrating macrophages of human renal cell carcinomas. Clin Cancer Res 2001;7:2145–51.
21. Li D, Xie K, Wolff R, Abbruzzese JL. Pancreatic cancer. Lancet 2004;363:1049–57.
22. Sener SF, Fremgen A, Menck HR, Winchester DP. Pancreatic cancer: a report of treatment and survival trends for 100,313 patients diagnosed from 1985–95, using the National Cancer Database. J Am Coll Surg 1999;189:1–7.
23. Ohtsubo K, Watanabe H, Yamaguchi Y, et al. Abnormalities of tumor suppressor gene p16 in pancreatic carcinoma: immunohistochemical and genetic findings compared with clinicopathological parameters. J Gastroenterol 2003;38:663–71.
24. Biankin AV, Morey AL, Lee CS, et al. DPC4/Smad4 expression and outcome in pancreatic ductal adenocarcinoma. J Clin Oncol 2002;206:4531–42.
25. Uehara H, Miyamoto M, Kato K, et al. Expression of pigment epithelium-derived factor decreases liver metastasis and correlates with favorable prognosis for patients with ductal pancreatic adenocarcinoma. Cancer Res 2004;64:3533–7.
26. Ikeda N, Adachi M, Taki T, et al. Prognostic significance of angiogenesis in human pancreatic cancer. Br J Cancer 1999;79:1553–63.
27. Shimamura T, Sakamoto M, Ino Y, et al. Dysadherin overexpression in pancreatic ductal adenocarcinoma reflects tumor aggressiveness: relationship to e-cadherin expression. J Clin Oncol 2003;21:659–67.
28. Iwamura T, Katsuki T, Ide K. Establishment and characterization of a human pancreatic cancer cell line (SUIT-2) producing carcinoembryonic antigen and carbohydrate antigen 19-9. Jpn J Cancer Res 1987;78: 54–62.
29. Ikeda Y, Ezaki M, Hayashi I, Yasuda D, Nakayama K, Kono A. Establishment and characterization of human pancreatic cancer cell lines in tissue culture and in nude mice. Jpn J Cancer Res 1990;81:987–93.
30. Ono M, Hirata A, Kometani T, et al. Sensitivity to gefitinib (Iressa, ZD1839) in non-small cell lung cancer cell lines correlates with dependence on the epidermal growth factor (EGF) receptor/extracellular signal-regulated kinase 1/2 and EGF receptor/Akt pathway for proliferation. Mol Cancer Ther 2004;3: 465–72.
31. Hirata A, Ogawa S, Kometani T, et al. ZD1839 (Iressa) induces antiangiogenic effects through inhibition of epidermal growth factor receptor tyrosine kinase. Cancer Res 2002;62:2554–60.
32. Jimi S, Shono T, Ono M, et al. Expression of matrix metalloproteinases 1 and 2 genes in a possible association with metastatic abilities of human pancreatic cancer cells. Int J Oncol 1997;10:623–8.
33. Nakao S, Kuwano T, Tsutsumi-Miyahara C, et al. Infiltration of COX-2-expressing macrophages is a prerequisite for IL-1β-induced neovascularization and tumor growth. J Clin Invest 2005;115:2979–91.
34. Ono M, Kawahara N, Goto D, et al. Inhibition of tumor growth and neovascularization by an anti-gastric ulcer agent, irsogladine. Cancer Res 1996;56: 1512–6.
35. Itokawa T, Nokihara H, Nishioka Y, et al. Anti-angiogenic effect by SU5416 is partly attributable to inhibition of Flt-1 receptor signaling. Mol Cancer Ther 2002;1:295–302.
36. Hiraoka N, Allen E, Apel IJ, Gyetko MR, Weiss SJ. Matrix metalloproteinases regulate neovascularization by acting as pericellular fibrinolysins. Cell 1998;95: 365–77.
37. Bergers G, Brekken R, McMahon G, et al. Matrix metalloproteinase-9 triggers the angiogenic switch during carcinogenesis. Nat Cell Biol 2000;2:737–44.
38. Le NT, Richardson DR. Iron chelators with high antiproliferative activity up-regulate the expression of a growth inhibitory and metastasis suppressor gene: a link between iron metabolism and proliferation. Blood 2004; 104:2967–75.
39. Fotovati A, Fujii T, Yamaguchi M, et al. 17β-Estradiol induces downregulation of Cap43/NDRG1/Drg-1, a putative differentiation-related and metastasis suppressor gene, in human breast cancer cells. Clin Cancer Res 2006;12:3010–8.

40. Yeo CJ, Cameron JL. Prognostic factors in ductal pancreatic cancer. Langenbecks Arch Surg 1998;383: 129–33.
41. Gebhardt C, Meyer W, Reichel M, Wunsch PH. Prognostic factors in the operative treatment of ductal pancreatic carcinoma. Langenbecks Arch Surg 2000;385: 14–20.
42. Schuch G, Kisker O, Atala A, Soker S. Pancreatic tumor growth is regulated by the balance between positive and negative modulators of angiogenesis. Angiogenesis 2002;5:181–90.
43. Baker CH, Solorzano CC, Fidler IJ. Blockade of vascular endothelial growth factor receptor and epidermal growth factor receptor signaling for therapy of metastatic human pancreatic cancer. Cancer Res 2002; 62:1996–2003.
44. Kuwahara K, Sasaki T, Kuwada Y, Murakami M, Yamasaki S, Chayama K. Expressions of angiogenic factors in pancreatic ductal carcinoma: a correlative study with clinicopathologic parameters and patient survival. Pancreas 2003;26:344–9.
45. Itakura J, Ishiwata T, Friess H, et al. Enhanced expression of vascular endothelial growth factor in human pancreatic cancer correlates with local disease progression. Clin Cancer Res 1997;3:1309–16.
46. Tsuzuki Y, Mouta Carreira C, Bockhorn M, Xu L, Jain RK, Fukumura D. Pancreas microenvironment promotes VEGF expression and tumor growth: novel window models for pancreatic tumor angiogenesis and microcirculation. Lab Invest 2001;81:1439–51.
47. Shi Q, Abbruzzese JL, Huang S, Fidler IJ, Xiong Q, Xie K. Constitutive and inducible interleukin 8 expression by hypoxia and acidosis renders human pancreatic cancer cells more tumorigenic and metastatic. Clin Cancer Res 1999;5:3711–21.
48. Kuwano M, Basaki Y, Kuwano T, et al. The clinical role of inflammatory cell infiltration in tumor angiogenesis—a target for antitumor drug development? In: New angiogenesis research, New York: Nova Science Publishers, Inc.; 2005. p. 157–70.
49. Lewis CE, Pollard JW. Distinct role of macrophages in different tumor microenvironments. Cancer Res 2006;66: 605–12.

The up-regulation of type I interferon receptor gene plays a key role in hepatocellular carcinoma cells in the synergistic antiproliferative effect by 5-fluorouracil and interferon-α

SHINJI OIE[1,3], MAYUMI ONO[1,2,4], HIROHISA YANO[4,5], YUICHIRO MARUYAMA[1,4], TADAFUMI TERADA[3], YUJI YAMADA[3,4], TAKATO UENO[4,6], MASAMICHI KOJIRO[4,5], KAZUYUKI HIRANO[7] and MICHIHIKO KUWANO[1,4]

[1]Station-II for Collaborative Research, [2]Department of Medical Biochemistry, Graduate School of Medical Sciences, Kyushu University, 3-1-1 Maidashi, Higashi-ku, Fukuoka 812-8582; [3]Drug Discovery Laboratory, TAIHO Pharmaceutical Co., Ltd., 1-27 Misugidai, Hanno-shi, Saitama 357-8527; [4]Research Center for Innovative Cancer Therapy, [5]Department of Pathology, [6]The Second Department of Internal Medicine, Kurume University School of Medicine, 67 Asahi-machi, Kurume, Fukuoka 830-0011; [7]Laboratory of Pharmaceutics, Gifu Pharmaceutical University, 5-6-1 Mitahora-higashi, Gifu-shi, Gifu 502-8585, Japan

Received March 10, 2006; Accepted April 26, 2006

Abstract. Combination therapy with interferon (IFN)-α and 5-fluorouracil (5-FU) has been reported to show an improved therapeutic efficacy in patients with advanced hepatocellular carcinoma (HCC) but the mechanism behind this has not been completely elucidated. We examined the molecular events underlying the antiproliferative effects of IFN-α and 5-FU in combination using six human HCC cell lines. When the antiproliferative effects of administering IFN-α and 5-FU together were analyzed using isobolograms, we found that the cell lines could be divided into two groups: the S-group containing three cell lines, which showed synergistic effects, and the A-group, containing the remaining three cell lines, which showed additive effects. Real-time RT-PCR and Western blot analyses revealed that the expression levels of type I IFN receptor subunits, IFNAR1 and IFNAR2, were specifically up-regulated by 5-FU in all three cell lines of the S-group with the exception of IFNAR2 in one cell line, but not in those of the A-group. IFN-α modulated the protein expression levels of six enzymes regulating sensitivity to 5-FU, but none of them were down- or up-regulated in the same way in all members of the S- or A-group. In conclusion, the 5-FU-induced modulation of IFN receptor expression could play a pivotal role in the therapeutic efficacy of IFN-α combined with 5-FU. Measuring the expression levels of IFN receptors, and their ability to be up-regulated, may be a promising method for selecting HCC patients for this type of combination therapy.

Correspondence to: Dr Shinji Oie, Station-II for Collaborative Research, Kyushu University, 3-1-1 Maidashi, Higashi-ku, Fukuoka 812-8582, Japan
E-mail: oh9906ie@qa2.so-net.ne.jp

Abbreviations: IFN-α, interferon α; 5-FU, 5-fluorouracil; HCC, hepatocellular carcinoma; IFNAR1, type I IFN receptor subunit 1; IFNAR2, type I IFN receptor subunit 2; FdUMP, 5-fluoro-2'deoxyuridine-5'-monophosphate; TS, thymidylate synthase; TP, thymidine phosphorylase; DPD, dihydropyrimidine dehydrogenase; OPRT, orotate phosphoribosyl transferase; UP, uridine phosphorylase; TK, thymidine kinase; RT-PCR, reverse transcription-polymerase chain reaction

Key words: interferon-α, 5-fluorouracil, combination therapy, synergism, interferon receptor, hepatocellular carcinoma

Introduction

Hepatocellular carcinoma (HCC), the most common primary liver cancer, is one of the most frequent and aggressive malignant tumors, and its incidence is increasing. The surgical resection of hepatic lesions is the most effective treatment for patients with HCC, and local therapeutic approaches, such as transcatheter arterial embolization (1), percutaneous transhepatic ethanol injection (2), microwave coagulation (3), and radiofrequency ablation (4) have also been reported to be effective. However, these therapies are still not effective for patients with advanced HCC, who are often not suitable for surgery and whose 5-year survival rate is extremely low (5). One chemotherapeutic strategy is combined chemotherapy with 5-fluorouracil (5-FU) and interferon (IFN)-α. Monden and colleagues have reported a beneficial therapeutic effect in a patient with recurrent HCC and multiple lung and bone metastases (6-8). However, this combined treatment was accompanied by increased toxicity, as manifested by an elevated incidence of mucositis and neurological and hematological side effects (9). It is therefore important to understand-

the exact mechanism of this combination therapy so that patients likely to respond can be selected and unnecessary side effects can be avoided.

5-FU has two major antitumor mechanisms: one involves its active metabolite 5-fluoro-2'-deoxyuridine-5'-monophosphate (FdUMP), inhibiting the activity of thymidylate synthase (TS) and consequently DNA synthesis; the other is related to the incorporation of 5-FU metabolite into RNA and DNA, thereby disrupting normal RNA processing and function. The sensitivity of cancer cells to 5-FU is often influenced by the enzymes affecting 5-FU metabolism, including dihydropyrimidine dehydrogenase (DPD), orotate phosphoribosyl transferase (OPRT), thymidine phosphorylase (TP), uridine phosphorylase (UP), and thymidine kinase (TK). In contrast, IFNs are divided into type I and type II. The human type I IFN family is composed of at least 14 structurally related IFN-α subtypes and single IFN-ß and IFN-ω subtypes. Type I IFNs have various biological activities, including antiviral, anti-proliferative, immunomodulatory (10-12), and anti-angiogenic effects (13,14), mediated by the type I IFN receptor. This receptor is composed of two functional transmembrane subunits, type I IFN receptor subunit 1 (IFNAR1) and subunit 2 (IFNAR2), cooperating to form a high-affinity receptor for all type I IFNs (15,16). IFNAR2 is the major binding subunit and IFNAR1 is necessary for the tight binding. Of these receptor molecules, the expression levels of the type I IFN receptor were closely correlated with the response rates to IFN treatment in patients with chronic hepatitis C (17), and overexpression of the IFNAR2 markedly increased the anti-proliferative activity of IFNs and their capacity to induce apoptosis (18), suggesting that the type I IFN receptor is a key molecule for the antitumor activity of IFN-α.

Concerning possible mechanisms behind IFN-α and 5-FU showing improved therapeutic efficacy, increased FdUMP concentrations, decreased protein level of TS, an increase in TS inhibition rate and TP activity, and an alteration in 5-FU pharmacokinetics by combined IFN-α have been reported (19-24). Eguchi *et al* have reported that augmentation of the antitumor effect of 5-FU by IFN-α might in part be attributable to the up-regulation of $p27^{Kip1}$ blocking cell cycle progression (25). However, none of these theories provide a consistent mechanism for the exact rationale of this combination therapy. Furthermore, almost all studies have assumed that IFN-α plays a role in modulating the antitumor activity of 5-FU.

In this study, we provide evidence that the modulation of IFN receptor expression by 5-FU is specifically associated with the improved efficacy rather than the cellular modulation of the enzymes that regulate the sensitivity to 5-FU by IFN-α.

Materials and methods

Drugs. Natural human IFN-α was purchased from Otsuka Pharmaceutical Co., Ltd. (OIF, Tokyo, Japan) and 5-FU was purchased from Kyowa Hakko Kogyo Co., Ltd. (5-FU Injection 250 Kyowa, Tokyo, Japan).

Cell lines. HCC cell lines, KIM-1, KYN-1, KYN-2, KYN-3, HAK-1A and HAK-1B (26-30), were grown in Dulbecco's modified Eagle's medium (Nissui Seiyaku Co., Tokyo, Japan) with 10% fetal bovine serum (FBS) (FETALCLONE III, Hyclone, UT, USA) in a humidified atmosphere of 5% CO_2 at 37°C.

Antiproliferation test. Cells were seeded into 96-well plates at 1,000 cells/0.1 ml/well and incubated overnight. On the following day, 100 µl aliquot containing IFN-α and 5-FU was added and cultured for a further 5 days. In study of schedule-dependent synergy, HCC cells were seeded into 12-well plates at 5,000 cells/1 ml/well. On the following day, 1-ml aliquot containing drugs was added. After a further 3 days, culture medium was exchanged for fresh medium including another drug and cultured for a further 3 days. The number of viable cells was estimated by activity of cellular dehyrogenases using WST-8 reagent (Cell Counting Kit-8, DOJINDO, Kumamoto, Japan) (31).

Isobologram analysis. To analyze the mode of interaction between 5-FU and IFN-α, the combined doses that reduced cell growth by 50% were plotted as isobolograms, according to the method of Steel and Peckham (32). The envelope of additivity surrounded by mode I (heteroaddition), IIa and IIb (isoaddition) curves, was constructed based on the dose-response curves of IFN-α and 5-FU alone. Thus, when the data points for the combined drugs fell within this envelope, the combined effect was judged to be additive. When the points fell in the area under the envelope of additivity, the combined effect was judged as synergistic, because in this case, 50% inhibition was produced by a lower concentration than predicted on an additive basis.

cDNA preparation and quantitative real-time RT-PCR. Total RNA was extracted using Isogen (Nippon Gene Co., Ltd., Tokyo, Japan) and reverse transcribed using a reverse transcription system (Promega Corp., Madison, WI) according to the manufacturer's instructions. RT-PCR was performed with an ABI PRISM 7300 (PE Applied Biosystems, Foster City, CA). The sequences of the primers and probes are shown in Table I, and those for IFNAR1, IFNAR2 and glyceraldehyde-3-phosphate dehydrogenase (GAPDH) were purchased from Applied Biosystems.

Western blotting. HCC cells were cultured with various concentrations of 5-FU or IFN-α. Total protein was extracted using protein extraction reagent (M-PER™, Pierce, Rockford, IL) supplemented with protease inhibitors (Halt™ protease inhibitor cocktail kit, Pierce). Cell lysates were subjected to SDS-PAGE and transferred to Immobilon-P transfer membranes (Millipore, Bedford, MA). After blocking, membranes were probed with anti-TS, -OPRT and -TP monoclonal and anti-DPD polyclonal antibodies (a gift from TAIHO Pharmaceutical Co., Ltd., Tokyo, Japan), monoclonal antibody against TK (abcam, Cambridge, UK), polyclonal antibodies against IFNAR1, IFNAR2 and UP (Santa Cruz Biotechnology, Santa Cruz, CA). The proteins were visualized using HRP-conjugated antibodies followed by enhanced chemiluminescence (Pierce). The intensity of luminescence was quantified using an image analysis system (LAS-1000, Fuji Film, Tokyo, Japan).

Silencing IFNAR1 and IFNAR2 genes. Stealth™ RNAis (Invitrogen™ Life Technologies, San Diego, CA) were used

Table I. Probe and primer pair sequences for six factors regulating 5-FU sensitivity.

Gene		Sequences
TS[a]	Probe:	5'-(FAM)TTCAGCTTCAGCGAGAACCCAGA(TAMRA)-3'
	Forward primer:	5'-GAATCACATCGAGCCACTGAAA-3'
	Reverse primer:	5'-CAGCCCAACCCCTAAAGACTGA-3'
DPD[b]	Probe:	5'-(FAM)TGCCCTCACCAAAACTTTCTCTCTTGATAAGGA(TAMRA)-3'
	Forward primer:	5'-AATGATTCGAAGAGCTTTTGAAGC-3'
	Reverse primer:	5'-GTTCCCCGGATGATTCTGG-3'
OPRT[c]	Probe:	5' (FAM)CTCCTTATTGCGGAAATGAGCTCCACC(TAMRA)-3'
	Forward primer:	5'-TCCTGGGCAGATCTAGTAAATGC-3'
	Reverse primer:	5'-TGCTCCTCAGCCATTCTAACC-3'
TP[d]	Probe:	5'-(FAM)CAGCCAGAGATGTGACAGCCACCGT(TAMRA)-3'
	Forward primer:	5'-CCTGCGGACGGAATCCT-3'
	Reverse primer:	5'-GCTGTGATGAGTGGCAGGCT-3'
UP[e]	Probe:	5'-(FAM)TGCTCCAACGTCACTATCATCCGCAT(TAMRA)-3'
	Forward primer:	5'-TGACTGCCCAGGTAGAGACTATCC-3'
	Reverse primer:	5'-AGACCTATCCCACCAGAAGTGC-3'
TK[f]	Probe:	5'-(FAM)TGGCCTGGATTCACGCCCTCTTG(TAMRA)-3'
	Forward primer:	5'-AGCCTTGGCCCACACTGA-3'
	Reverse primer:	5'-CCAGAGGTAGGAAGGGCTTTG-3'

[a]Thymidylate synthase; [b]dihydropyrimidine dehydrogenase; [c]orotate phosphoribosyl transferase; [d]thymidine phosphorylase; [e]uridine phosphorylase; and [f]thymidine kinase.

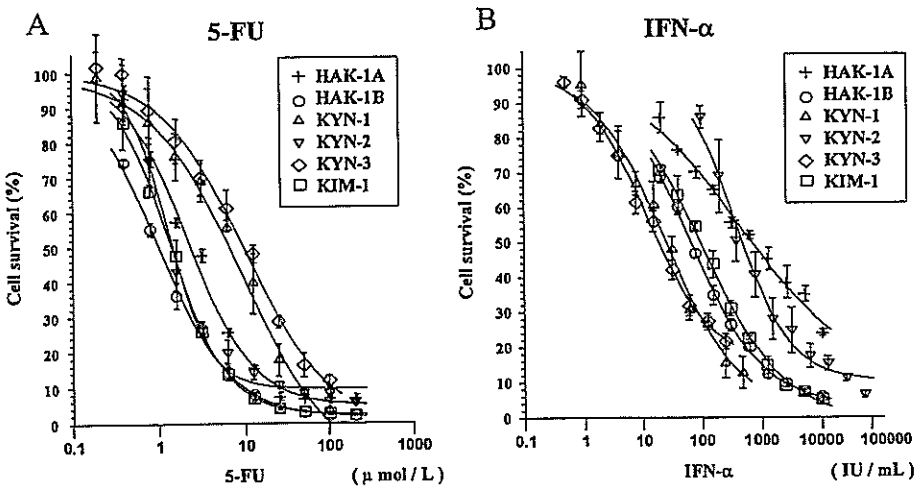

Figure 1. Antiproliferative effects of IFN-α and 5-FU in six HCC cell lines, HAK-1A, HAK-1B, KYN-1, KYN-2, KYN-3, and KIM-1. Cells were exposed to drugs for 5 days. Curves show the fitted dose-response curves for 5-FU (A) and IFN-α (B). Assays were carried out in quadruplicate. Data points represent the mean ± SD of the cell survival ratio relative to that of untreated cells, taken as 100%. Experiments were repeated twice with essentially similar results.

to knock down IFNAR1 (j03171_stealth_189) and IFNAR2 (x89772_stealth_1054) expression. Sub-confluent KYN-1 cells were cultured overnight in Opti-MEM I medium, then 40 nmol/l siRNA and Lipofectamine™ 2000 (Invitrogen™ Life Technologies) were applied according to the manufacturer's instructions. After 4 h, cells were harvested from the culture plates and seeded into 96-well plates. After a further 8-h incubation, IFN-α was applied and cells were cultured for 5 more days. The numbers of cells were estimated by WST-8 method (31).

Results

Antiproliferative effects of IFN-α and 5-FU in six HCC cell lines. When the antiproliferative effects of IFN-α and 5-FU on six HCC cell lines were examined, the growth inhibition seen

Table II. Relative mRNA expression levels of type I IFN receptor subunits and six factors regulating sensitivity to 5-FU in six HCC cell lines.

Cell line	Relative mRNA levels [a]								IC_{50}[j]	
	IFNAR1[b]	IFNAR2[c]	TS[d]	DPD[e]	OPRT[f]	TP[g]	UP[h]	TK[i]	IFN-α (IU/ml)	5-FU (μmol/l)
HAK-1A	23	5	100	1	100	6	16	91	700	2.3
HAK-1B	100	100	15	59	84	100	100	43	66	1.0
KYN-1	99	54	67	100	71	15	94	99	25	7.2
KYN-2	5	13	9	4	38	34	2	92	490	1.4
KYN-3	27	14	66	13	55	31	36	92	19	9.6
KIM-1	38	27	20	87	42	55	19	100	94	1.4

[a]The mRNA levels were examined by quantitative real-time RT-PCR and normalized with GAPDH. Relative mRNA level shows the average of the ratio relative to the highest level in six HCC cell lines of 100 in respective factor in triplicate determinations. [b]Type I interferon receptor subunit 1; [c]type I interferon receptor subunit 2; [d]thymidylate synthase; [e]dihydropyrimidine dehydrogenase; [f]orotate phosphoribosyl transferance; [g]thymidine phosphorylase; [h]uridine phosphorylase, and [i] thymidine kinase. [j]IC_{50}, drug concentration reducing the cell growth to 50% of that of non-treated cells. Cytotoxicity tests were carried out in quadruplicate.

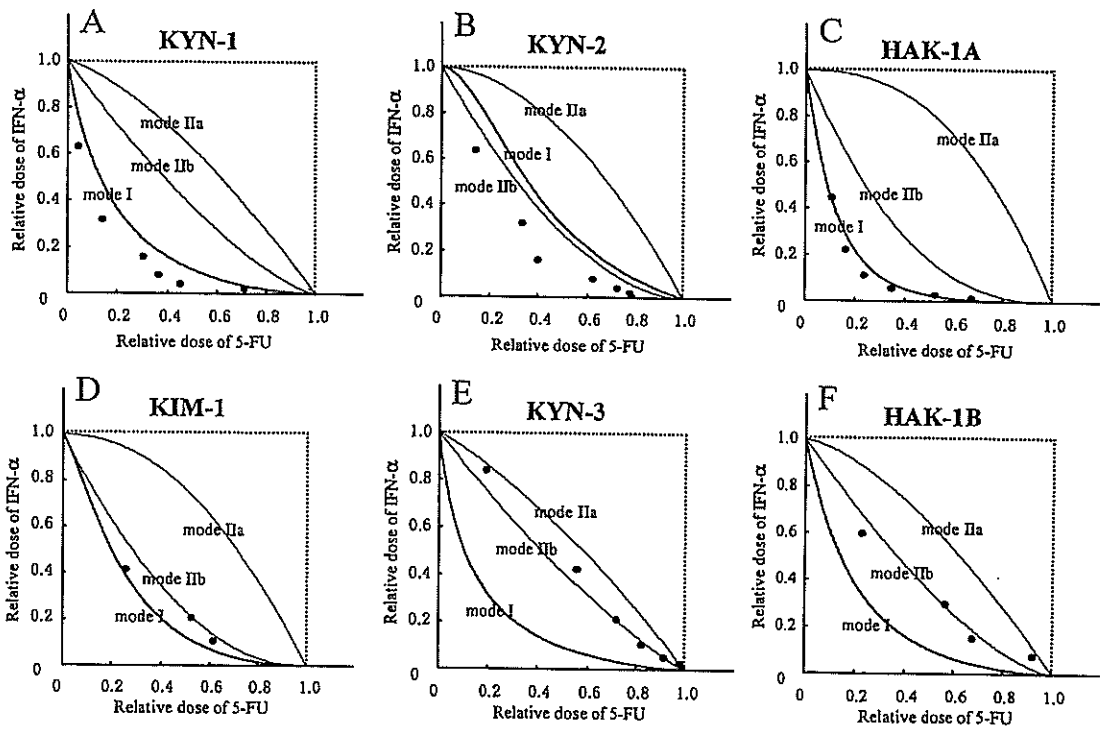

Figure 2. Combination effects of IFN-α and 5-FU. Isobologram analysis of IFN-α and 5-FU against six HCC cell lines. Cells were exposed to IFN-α and 5-FU for 5 days simultaneously. The area surrounded by the outer 2 curves of Mode I, IIa and IIb curves is the envelope of additivity. Relative doses of the drugs were calculated as concentration of 5-FU/IC_{50} of 5-FU and concentration of IFN-α/IC_{50} of IFN-α. Closed circles represent combined concentrations of 5-FU and IFN-α that inhibited cell growth by 50%. Assays were carried out in quadruplicate. Experiments were repeated twice with essentially similar results.

in all HCC cell lines was dose-dependent (Fig. 1). The HCC cell lines showed varied sensitivities to IFN-α, with IC_{50} values over a 25-fold range, from 19 to 700 IU/ml (Table II). KIM-1, KYN-1, KYN-3, and HAK-1B were highly sensitive to IFN-α with IC_{50} values below 100 IU/ml, while HAK-1A and KYN-2 appeared to be more resistant with IC_{50} values of 700 and 490 IU/ml, respectively. KYN-1 and KYN-3 responded weakly to 5-FU with IC_{50} values of 7.2 and 9.6 μmol/l, respectively, while the remaining four HCC cell lines were approximately three times more sensitive to 5-FU.

Expression of type I IFN receptor and factors regulating 5-FU sensitivity in six HCC cell lines. Table II shows the relative levels of basal mRNAs for IFNAR1, IFNAR2 and factors regulating sensitivity to 5-FU, with an arbitrary maximum value of 100. The mRNA levels of IFNAR1 were highest in

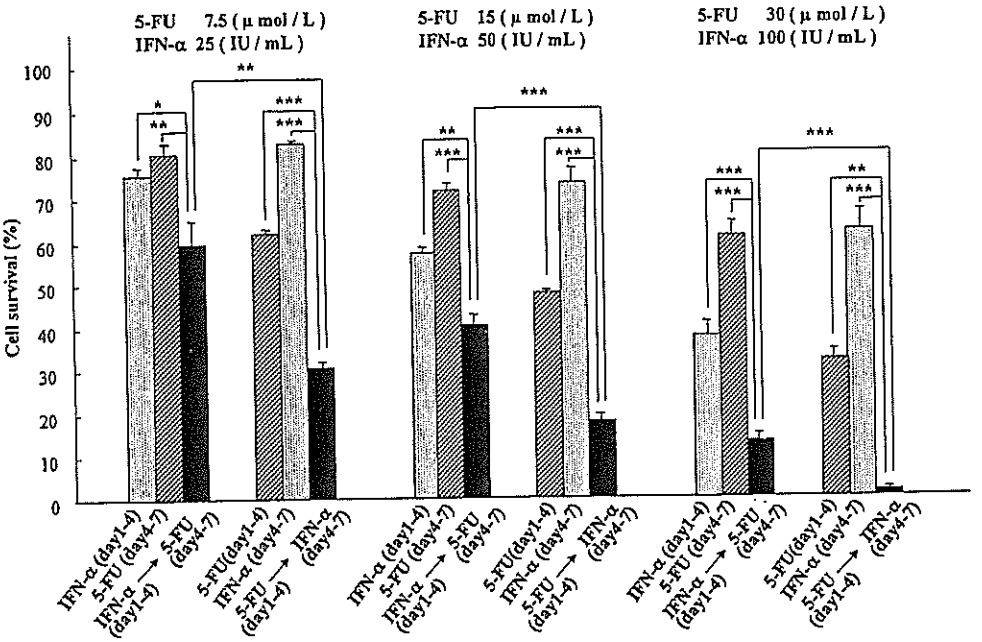

Figure 3. Schedule dependency of synergism of IFN-α and 5-FU. KYN-1 cells were seeded on day 0 and exposed to IFN-α or 5-FU for 3 days (day 1-4). On day 4, culture medium was removed and washed with PBS three times and fresh medium containing another drug was added. Cells were cultured for a further 3 days (day 4-7). The number of viable cells was estimated using the WST-8 assay. Experiments were carried out in triplicate independently. The columns show the mean value and bars represent SDs. Dotted column, IFN-α alone; striped column, 5-FU alone; solid column, sequential treatment of 5-FU and IFN-α. *P<0.05, **P<0.01, ***P<0.001; statistically significant difference between the indicated data points by Welch's test.

the IFN-α-sensitive cell lines HAK-1B and KYN-1, while those in the other four HCC lines, which included both IFN-α-sensitive and resistant lines, were only 5-40% of their levels in HAK-1B. As for IFNAR-1, the levels of IFNAR-2 mRNA were relatively higher in HAK-1B and KYN-1. Moreover, both IFN-α-resistant cell lines, HAK-1A and KYN-2, had relatively lower levels of IFNAR-1 and IFNAR-2 mRNAs, while the other IFN-α-sensitive cell lines had relatively higher levels of mRNA for both subunits.

Of the six factors regulating sensitivity to 5-FU, low levels of TS and DPD and high levels of OPRT, TP, UP and TK render cancer cells sensitive to 5-FU in *in vitro* assays. Cellular TS mRNA levels were relatively high in two 5-FU-resistant lines, KYN-1 and KYN-3, while DPD mRNA levels were high only in KYN-1 cells. Cellular TP mRNA levels were relatively low in the 5-FU-resistant KYN-1, but high in the 5-FU-sensitive HAK-1B cells. However, overall there was no clear association between the cellular mRNA levels of each factor and the 5-FU sensitivity of the six HCC lines.

Combined effect of IFN-α and 5-FU on six HCC cell lines. The isobologram method yielded three curves, Mode I, Mode IIa and Mode IIb. All of the data points for combined treatments against KYN-1 and KYN-2 cell lines, and three out of six data points for HAK-1A, fell in the area suggesting a synergistic effect and the other three points for HAK-1A cells were almost on the mode I curve (Fig. 2A and C). Therefore the combined effect of IFN-α and 5-FU on these three cell lines was judged to be synergistic. By contrast, all of the data points for combined treatments of HAK-1B, KYN-3, and KIM-1 cells fell within the envelope of additivity, and the combined effects on these cell lines were judged to be additive (Fig. 2D and F). Based on these results, we separated the six cell lines into two groups: the S-group, showing synergistic responses, and consisting of KYN-1, KYN-2, and HAK-1A, and the A-group, characterized by additive responses, and consisting of HAK-1B, KYN-3, and KIM-1.

As shown in Fig. 3, schedule-dependent interactions between IFN-α and 5-FU were examined using KYN-1 cells showing synergistic effect with simultaneous treatment of IFN-α and 5-FU. Sequential exposure to 5-FU followed by IFN-α showed much stronger antiproliferative effect than the reverse sequence at all tested concentration sets of 5-FU and IFN-α.

Effect of IFN-α on protein expression of factors regulating 5-FU sensitivity. The metabolism of 5-FU is shown in Fig. 4A. The antitumor effects of 5-FU primarily depend on levels of its metabolic enzymes in *in vitro* study. We selected six enzymes, TS, DPD, OPRT, TP, UP and TK, that were reported to be closely associated with sensitivity and/or resistance to 5-FU. We examined their protein levels in these six cell lines when treated with IFN-α at 500 IU/ml for 48 h (Fig. 4B). The expression levels of TS, OPRT and TK were down-regulated after treatment with IFN-α for 48 h, not only cell lines in the S-group, but also in the A-group. By contrast, treatment with IFN-α resulted in a 3-fold increase in DPD protein level in KYN-3 cells. We also observed an up-regulation of TP in IFN-α treated KYN-1 and HAK-1A cells, both in the S-group, by 6.9- and 2.8-fold respectively. However, none of the six factors regulating sensitivity to 5-FU was consistently modulated in response to IFN-α in all of the S-group or all of the A-group cell lines.

Effect of 5-FU on expression of IFNAR1 and IFNAR2 in six HCC cell lines. The relative mRNA levels of IFNAR1 and

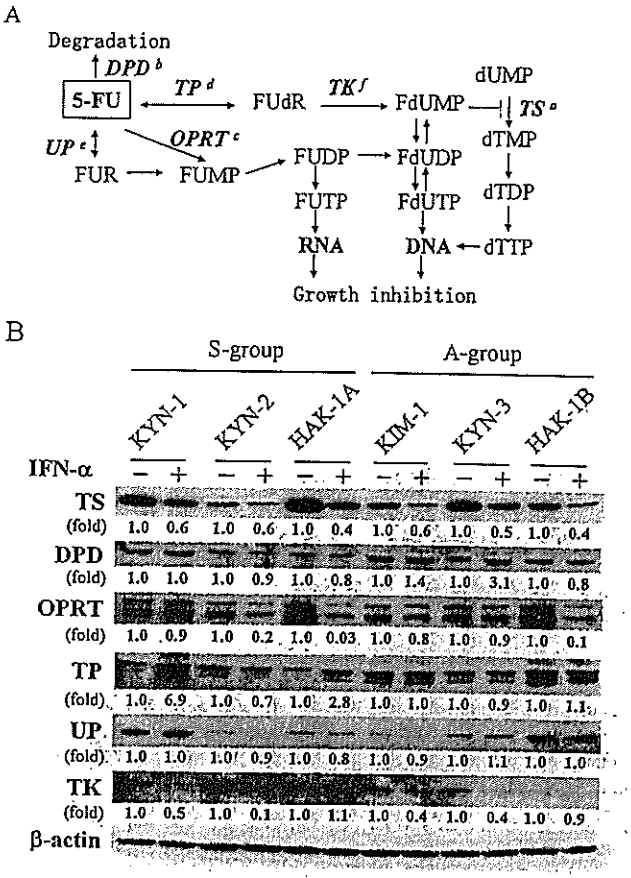

Figure 4. Effect of IFN-α on factors regulating sensitivity to 5-FU. (A) Metabolism of 5-FU. [a]TS, thymidylate synthase; [b]DPD, dihydropyrimidine dehydrogenase; [c]OPRT, orotate phosphoribosyl transferase; [d]TP,thymidine phosphorylase; [e]UP, uridine phosphorylase; [f]TK,thymidine kinase; FUdR, 5-fluoro-2'-deoxyuridine; FdUMP, 5-fluoro-2'-deoxyuridine-5'-monophosphate; FdUDP, 5-fluoro-2'-deoxyuridine-5'-diphosphate; FdUTP, 5-fluoro-2'-deoxyuridine-5'-triphosphate; FUR, 5-fluorouridine; FUMP, 5-fluorouridine-5'-monophosphate; FUDP, 5-fluorouridine-5'-diphosphate; FUTP, 5-fluorouridine-5'-triphosphate. TS is a target enzyme of active metabolite FdUMP from 5-FU, and DPD inactivates 5-FU. OPRT, TP, UP and TK were concerned with conversion of 5-FU to its active form. Low levels of TS and DPD and high levels of OPRT, TP, UP and TK render cancer cells sensitive to 5-FU in *in vitro* assays. (B) Protein expression of six enzymes after 48-h treatment with 500 IU/ml IFN-α were determined by Western blot analysis. Values underneath the bands represent the relative density to that of drug untreated cells, taken as 1.0. Cell lines in the S-group showed synergistic effect, and those in the A-group showed additive effect with combination of IFN-α and 5-FU.

IFNAR2 in 5-FU-treated HCC cells, compared to untreated cells, are shown in Fig. 5. In HAK-1A, KYN-1 and KYN-2 in the S-group, treatment with 5-FU induced an approximately 4-fold increase in IFNAR-1 mRNA levels when compared to untreated cells (Fig. 5A). By contrast, there appeared only a slight or no increase in IFNAR-1 mRNA in KIM-1, KYN-3, and HAK-1B in the A-group. We observed a 2.5- to 3-fold increase in IFNAR2 mRNA in KYN-1 and HAK-1A, but not in KYN-2 in the S-group by 5-FU. By contrast, there appeared no increase of IFNAR2 mRNA by 5-FU in KIM-1, KYN-3, and HAK-1B cells in the A-group (Fig. 5B). Time-dependent kinetics for the expression of both type I IFN receptor subunits showed a marked increase in IFNAR1 and IFNAR2 mRNA levels at 3 h in KYN-1 cells, but not in KYN-3 cells when treated with 5-FU (Fig. 6A and B). In KYN-1 cells, Western blot analysis also showed an approximate 4-fold increase in protein levels of IFNAR1, 24 h after exposure to 5-FU (Fig. 6C). Treatment of KYN-1 cells with 5-FU induced an approximate 7-fold increase in IFNAR2 protein. In contrast, in KYN-3 cells in the A-group, the levels of the IFNAR2-related molecules R2 were not increased by 5-FU treatment (Fig. 6D).

Effect of knockdown of IFNAR1 and IFNAR2 by siRNA on antiproliferative effect of IFN-α. We next examined whether cellular levels of IFNAR1 and/or IFNAR2 were closely associated with IFN-α-induced antiproliferative effect in KYN-1 and KYN-3. Cellular levels of IFNAR1 and IFNAR2 proteins were markedly reduced by the relevant siRNAs, but not by scrambled RNAs (Fig. 7A). Moreover, the antiproliferative effect of IFN-α on both KYN-1 and KYN-3 cells was abrogated by knockdown of either IFNAR1 or IFNAR2, while the scrambled RNAs had no effect (Fig. 7B). Quantitative analysis of the cell survival curves of KYN-1 revealed that the knockdown of IFNAR1 and IFNAR2 increased the IC_{50} values for IFN-α, by 7-fold (231 IU/ml) and 5-fold (158 IU/ml) respectively, compared to the IC_{50} values (31 IU/ml) for cells untreated with siRNAs and treated with scramble RNAs (Fig. 7C and Table III). In KYN-3 cells, the knockdown of IFNAR1 and IFNAR2 increased the IC_{50} values for IFN-α from 21 IU/ml for untreated control cells to over 1000 IU/ml respectively. The antiproliferative activity of IFN-α

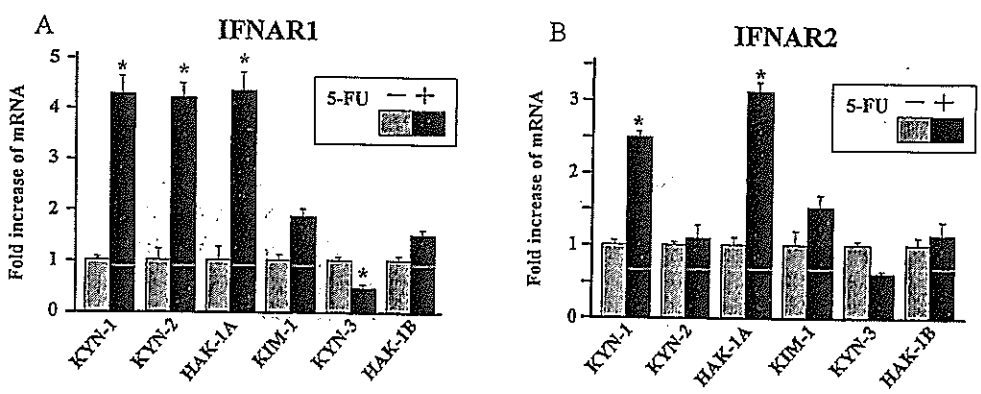

Figure 5. Expression of IFNAR1 and IFNAR2 mRNA, in HCC cells treated with 5.0 μmol/l 5-FU for 3 h. The increases in mRNA are shown relative to the initial level, taken as 1.0. Dotted and black columns show the mean mRNA levels in drug-untreated and 5-FU-treated cells, respectively. (A) IFNAR1, (B) IFNAR2. Determinations were carried out in triplicate, and bars represent the SDs. Experiments were repeated twice with essentially similar results. *Difference is >2-fold and statistically significant by Welch's test ($P<0.05$) as compared with untreated cells.